Fish and Shellfish Immunology 161 (2025) 110279

Contents lists available at ScienceDirect

Fish and Shellfish Immunology

journal homepage: www.elsevier.com/locate/fsi

Full length article

A novel antimicrobial peptide Larimicin$_{78\text{-}102}$ from large yellow croaker (*Larimichthys crocea*) shows potent antibacterial activity *in vitro* and enhances resistance to *vibrio fluvialis* infection *in vivo*

Zhenzhen Zhou [a], Fangyi Chen [a,b,c,*], Hua Hao [a,b,c], Ke-jian Wang [a,b,c,**]

[a] State Key Laboratory of Marine Environmental Science, College of Ocean and Earth Sciences, Xiamen University, Xiamen, 361102, China
[b] State-Province Joint Engineering Laboratory of Marine Bioproducts and Technology, College of Ocean and Earth Sciences, Xiamen University, Xiamen, 361102, China
[c] Fujian Innovation Research Institute for Marine Biological Antimicrobial Peptide Industrial Technology, College of Ocean and Earth Sciences, Xiamen University, Xiamen, 361102, China

ARTICLE INFO

Keywords:
Larimichthys crocea
Antimicrobial peptide
Larimicin$_{78\text{-}102}$
Antimicrobial activity
Anti-*Vibrio fluvialis* infection

ABSTRACT

Antimicrobial peptides (AMPs) are considered a key component of innate immunity, playing a vital role in host defense. In the study, a novel functional gene, named *Larimicin*, was identified from large yellow croaker *Larimichthys crocea*. The *Larimicin* gene was widely distributed in multiple tissues of healthy *L. crocea* and was significantly induced in the liver after *Vibrio alginolyticus* or *Vibrio parahaemolyticus* infection. Larimicin$_{78\text{-}102}$, a truncated peptide derived from *Larimicin*, showed broad-spectrum antimicrobial activity and a binding affinity with LPS. It exhibited effective bactericidal activity against the common aquatic pathogens *Vibrio fluvialis*, *Pseudomonas fluorescens,* and *Pseudomonas putida*. It also showed anti-biofilm activity against three aquatic pathogens. Moreover, Larimicin$_{78\text{-}102}$ disrupted the integrity of the outer and inner membranes, resulting in ATP leakage and intracellular ROS accumulation, which ultimately led to bacterial cell death. Larimicin$_{78\text{-}102}$ exhibited good thermal stability and cation tolerance, with no obvious cytotoxicity or hemolytic activity. Notably, Larimicin$_{78\text{-}102}$ significantly improved the survival rate of *L. crocea* infected with *V. fluvialis*, raising it to 95 %, indicating its anti-infective role *in vivo*. In addition, Larimicin$_{78\text{-}102}$ significantly reduced the expression of the pro-inflammatory cytokines *TNF-α* and *IL-1β*, while up-regulating the anti-inflammatory factor *IL*-4 mRNA level. It also elevated the expression levels of *piscidin*, *hepcidin*, and *lysozyme*, as well as enhanced the enzymatic activity of lysozyme. Taken together, Larimicin$_{78\text{-}102}$ is a potential antibacterial agent for use in aquaculture to combat *V. fluvialis* infection diseases in the future.

1. Introduction

Bacterial pathogens, including *Vibrio*, *Pseudomonas*, *Aeromonas* and *Nocardia* species, are common causative agents in aquaculture, which can cause mass mortalities in a short period of time and significant economic losses [1,2]. Among the pathogens infecting aquatic animals, *Vibrio* species are the most common group. *Vibrios*, widely distributed in estuarine and marine environments, are Gram-negative bacteria that are pathogenic to aquatic organisms [3]. For example, *Vibrio alginolyticus*, *Vibrio harveyi*, and *Vibrio parahaemolyticus* are prevalent pathogens in marine animals such as fish, shrimp and shellfish, causing severe mortality [4–6]. These pathogens have been isolated from large yellow croaker *Larimichthys crocea* [1]. Additionally, it is reported that *Vibrio fluvialis* is also a common pathogen in fish and shrimp [7,8], and it was isolated from large yellow croaker as well [9]. Vibriosis caused by pathogenic *Vibrio* species is the most common bacterial disease in aquaculture with the highest incidence rate [10,11]. Antibiotics like tetracycline, oxytetracycline, nitrofurans, sarafloxacin, trimethoprim and quinolones are commonly used in aquaculture to prevent and treat vibriosis [12]. However, prolonged and widespread use of antibiotics can cause various negative impacts, including antibiotic residues and emergence of drug-resistant bacteria in aquaculture [13], which

* Corresponding author. State Key Laboratory of Marine Environmental Science, College of Ocean & Earth Sciences, Xiamen University, Xiamen, Fujian, 361102, China.
** Corresponding author. State Key Laboratory of Marine Environmental Science, College of Ocean & Earth Sciences, Xiamen University, Xiamen, Fujian, 361102, China.
E-mail addresses: chenfangyi@xmu.edu.cn (F. Chen), wkjian@xmu.edu.cn (K.-j. Wang).

https://doi.org/10.1016/j.fsi.2025.110279
Received 18 January 2025; Received in revised form 10 March 2025; Accepted 13 March 2025
Available online 13 March 2025

Table 1
Sequences of primers used in this study.

Primer name	Primer sequence (5′–3′)	Purpose
Larimicin-F	ATTCACATATCAGCTCTTCA	RT primer
Larimicin -R	CTGATGACCACTTTATCCCCT	RT primer
UPM-Long	CTAATACGACTCACTATAGGGCAAGCAGTGGTATCAACGCAGAGT	RACE primer
UPM-Short	CTAATACGACTCACTATAGGGC	RACE primer
Larimicin-3′-F1	CTGCAGCGTTGCCTCACTTG	3′ RACE primer (outer)
Larimicin-3′-F2	TTTTGCTGTGCAGCACCTCG	3′ RACE primer (inner)
Larimicin-5′-R1	GCCTGTTCGTGATACGCTGC	5′ RACE primer (outer)
Larimicin-5′-R2	CCTCTGCGGTAGGTTCACCA	5′ RACE primer (inner)
M13-47F	CGCCAGGGTTTTCCCAGTCACGAC	Insert verification and sequencing
M13-48R	AGCGGATAACAATTTCACACAGGA	Insert verification and sequencing
Larimicin-qPCR-F	CACGTCGCCGTTAAACACAG	qPCR
Larimicin-qPCR-R	TGCTGCACAGCAAAATGTCC	qPCR
TNF-α-F	TAAGAACACCTACGAGACCATCCTGC	qPCR
TNF-α-R	CTCTTCTCCATCACCGTCTTCAGTTT	qPCR
IL-1β-F	GGCTGAACCTTAGTACCCTTG	qPCR
IL-1β-R	GATGTTGAAGTTTCTGTGGCG	qPCR
IL-4-F	TCATCAGAACCAGACCAG	qPCR
IL-4-R	TTATCCGCACATTCAGAGA	qPCR
piscidin-F	CGGGGAGTGTCTTGGAGG	qPCR
piscidin-R	CCAGCGAGCTCCATACCAT	qPCR
hepcidin-F	CACATCCAACCATCAGACCAG	qPCR
hepcidin-R	GAAGACAAATGAAGGCGAGCA	qPCR
lysozyme-F	GCACTAACTAATGGATGGGGAGACT	qPCR
lysozyme-R	CTGGCAACAACATCATTGGAGTAG	qPCR
ubiquitin-F	TGGAGGATGGACGCACACTG	qPCR
ubiquitin-R	GCAGACGGGCATAGCACTTG	qPCR
β-actin-F	CTACGAGGGTTATGCCCTGCC	qPCR
β-actin-R	TGAAGGAGTAACCGCGCTCTGT	qPCR

seriously affect the health of both animal and human [14]. Therefore, there is an urgent need to develop novel, effective and environmentally friendly antibacterial agents.

Antimicrobial peptides (AMPs) are important immune effectors in organisms, which produce rapid immune responses against pathogenic microorganisms, such as bacteria, fungi, viruses and parasites [15,16]. AMPs are usually extracted from organisms, or peptide derivatives, or synthetic. They are characterized by key structural features, including positive charge, hydrophobicity, and amphipathicity [17]. They can interact with anionic groups on microbial membranes, inducing cell destruction and leakage of cell contents, or targeting cytoplasmic components to kill bacteria [18]. Moreover, AMPs have multiple mechanisms of action, which reduce the chances of bacterial resistance [19]. AMPs are considered to be the most promising substitutes to antibiotics in aquaculture.

To date, a variety of AMPs have been found in multiple species, such as animal, plant, bacteria, and fungi. Among them, only a small number of AMPs have been from marine animals [20,21]. In view of the complex aquatic environment, marine animals-derived AMPs will expand the options for feasible antimicrobial agents against various pathogens. Large yellow croaker has become the highest production mariculture economic fish in China, reaching 257683 tons in 2022 (2023 China Fisheries Statistical Yearbook). At present, a variety of AMPs have been identified from large yellow croaker, such as piscidins [22], hepcidins [23], β-defensin [24], and NK-lysins [25]. Piscidins and hepcidin showed pronounced activity against *Cryptocaryon irritans* [22,26]. Hepcidin, LcBD2 and Lc-NK-lysin-1 exhibited significant antimicrobial effects on various *Vibrio* species, such as *V. alginolyticus* and *V. harveyi* [23–25]. However, the *in vivo* anti-infective effects of the above AMPs have not been elucidated, hindering their application as antimicrobial agents in animals. Given the limited number of available AMPs, further screening for novel candidates is essential for controlling vibriosis in aquaculture.

In this study, we identified a novel immune-associated functional gene from large yellow croaker, named *Larimicin*. The full-length cDNA sequences of the gene were cloned by RACE-PCR, and its expression profile was examined by qPCR. According to $CAMP_{R4}$ prediction, $Larimicin_{78\text{-}102}$, a truncated peptide derived from *Larimicin*, was synthesized using chemical methods and evaluated for its antimicrobial activity. The antimicrobial mechanism of $Larimicin_{78\text{-}102}$ was further explored, and its anti-infective efficacy was evaluated using a large yellow croaker infection model. The mRNA expression of three inflammatory factors (*TNF-α*, *IL-1β*, and *IL-4*) and three AMP genes (*piscidin*, *hepcidin*, and *lysozyme*) in the intestine and spleen of *L. crocea* were analyzed using qPCR. The enzymatic activity of lysozyme was also measured. This study would provide valuable insights for the development of effective and biocompatible anti-*V. fluvialis* agents.

2. Materials and methods

2.1. Microorganism strains and cell lines

Staphylococcus epidermidis (CGMCC No. 1.4260), *Staphylococcus aureus* (CGMCC No. 1.2465), *Escherichia coli* (CGMCC No. 1.2389), *Pseudomonas putida* (CGMCC No. 1.3136), *Pseudomonas aeruginosa* (CGMCC No. 1.2421), *Pseudomonas fluorescens* (CGMCC No. 1.3202), *Pseudomonas stutzeri* (CGMCC No. 1.1803), *Shigella flexneri* (CGMCC No. 1.1868), *Acinetobacter baumannii* (CGMCC No. 1.6769), *V. fluvialis* (CGMCC No. 1.1609), *V. alginolyticus* (CGMCC No. 1.1833), *V. parahaemolyticus* (CGMCC No. 1.1997), *Cryptococcus neoformans* (CGMCC No. 2.1563) were bought from the China General Microbiological Culture Collection Center (CGMCC).

The study utilized several cell lines, including mouse macrophages (RAW264.7), human embryonic kidney cells (HEK-293T), zebrafish embryonic cells (ZF4) and large yellow croaker kidney cells (LYCK). HEK-293T cells, obtained from Stem Cell Bank at the Chinese Academy of Sciences (Shanghai, China), were cultured in DMEM (Gibco, USA) medium with 10 % fetal bovine serum (FBS) (Gibco, USA) at 37 °C under 5 % CO_2. Similarly, RAW264.7 cells, sourced from National Infrastructure of Cell Line Resource (Beijing, China), were maintained in DMEM (Gibco, USA) medium supplemented with 10 % FBS (Gibco, USA) at the same temperature and CO_2 concentration. ZF4 cells came from China Zebrafish Resource Center (Wuhan, China) and were grown in DMEM/F12 (1:1) (Gibco, USA) medium with 10 % FBS (Gibco, USA) at 28 °C

under 5 % CO_2. LYCK cells were bought from China Center for Type Culture Collection (Wuhan, China) and cultured in M199 (Basal, China) medium with 20 % FBS (Gibco, USA) at 28 °C with 5 % CO_2.

2.2. Animals, challenge and tissue collection

Healthy large yellow croaker (30 ± 10 g) used for the study was obtained by artificial breeding in Ningde City in Fujian province, China. These fish were acclimated in a tank at 25 °C for 5 days. Four randomly selected fish were dissected after anesthesia with 0.5 % ethyl 3-aminobenzoate methanesulfonate (MS-222, Macklin, China). Tissues, including the brain, head kidney, hind kidney, spleen, liver, intestine, heart, muscle, stomach, and gills, were collected and stored at −80 °C.

Considering the difficulty of offshore cultivation for *L. crocea*, the challenge experiment was done in the field laboratory where a short distance reaches to the raising farm. Large yellow croaker was acclimatized in a tank at 25 °C for 5 days. A total of 100 large yellow croakers were divided into five distinct groups, one control group injected with PBS and four experimental groups, each treated with different concentrations of *V. alginolyticus* (3.125×10^6 CFU/100 μL, 6.25×10^6 CFU/100 μL, 1.25×10^7 CFU/100 μL, and 2.5×10^7 CFU/100 μL). Six groups of large yellow croakers were created, five of which were intraperitoneally infected with different concentrations of *V. parahaemolyticus* (7.5×10^6 CFU/100 μL, 1.5×10^7 CFU/100 μL, 3×10^7 CFU/100 μL, 6×10^7 CFU/100 μL, and 1.2×10^8 CFU/100 μL), and one group was injected with PBS as the control. There were 20 fish in each group. The survival rate of fish was recorded at different time. The survival curves were plotted using GraphPad Prism 8.0. The 50 % lethal concentration (LC_{50}) at 168 h was determined using Probit analysis.

For the challenge experiment, 72 large yellow croakers (30 ± 10 g), acclimatized for 5 days, were randomly divided into three groups (24 fish in each group): the control group injected with PBS (100 μL per fish), *V. alginolyticus* infection group (1.72×10^7 CFU/100 μL, 100 μL per fish) and *V. parahaemolyticus* infection group (6.5×10^7 CFU/100 μL, 100 μL per fish). All groups were then infected through intraperitoneal injection. The livers from three individuals in each group were obtained at different time points (3, 9, 12, 24, 48, 72, 96, and 120 h post-infection) after anesthesia with 0.5 % ethyl 3-aminobenzoate methanesulfonate (MS-222, Macklin, China) and stored at −80 °C.

2.3. Gene cloning and qPCR

Total RNA was extracted using the Trizol reagent (Invitrogen, USA), and cDNA was synthesized using the SuperScript™ III Reverse Transcriptase kit (Promega, USA). A pair of primers for *Larimicin* can be listed in Table 1. It was used to amplify the *Larimicin* gene through polymerase chain reaction (PCR). To obtain the partial sequence of *Larimicin*, PCR was performed using 2 × Taq Master Mix (Dye Plus) (Vazyme, China) in a total reaction volume of 50 μL, containing 1 μL of spleen cDNA as the template, 2 μL of *Larimicin*-F/R primers, 25 μL of 2 × Taq Master Mix (Dye Plus), and 20 μL of Milli-Q water. The PCR procedure was as follows: 94 °C, 5 min; 30 cycles of 94 °C, 30 s, 60 °C, 30 s, 72 °C, 1 min; 72 °C, 5 min. The SMARTer RACE 5'/3′ Kit (TaKaRa, Japan) was employed to amplify the full-length sequence of *Larimicin* using nest PCR. The primers *Larimicin*-3′-F1 and *Larimicin*-5′-R1 were used to amplify the 3′ and 5′ cDNA ends of *Larimicin* in the first round of PCR. The second round of PCR was performed using primers *Larimicin*-3′-F2 and *Larimicin*-5′-R2. The touchdown PCR conditions were set as follows: 94 °C, 5 min; 30 cycles of 94 °C, 30 s, 66 °C (−0.5 °C/cycle), 30 s, 72 °C, 2 min 20 s; 72 °C, 5 min. The PCR product was separated on a 1.2 % agarose gel, purified, cloned into the pMD18-T vector (TaKaRa, Japan), and transformed into DH5α competent cells. Positive colonies were screened and sequenced (Xiamen Borui Biological Technology Company, Xiamen, China).

The expression levels of *Larimicin*, three inflammatory genes (*TNF-α*, *IL-1β* and *IL-4*), and three AMP genes (*piscidin*, *hepcidin* and *lysozyme*) were analyzed by quantitative PCR (qPCR) on an CFX Opus 384 (BIO-RAD, Singapore). Moreover, the housekeeping gene *β-actin* and *ubiquitin* were used as an internal reference. The PCR program was set according to the instructions of HiScript III RT SuperMix for qPCR (+gDNA wiper) (Vazyme, China). The experimental data were analyzed using the $2^{-\triangle\triangle Ct}$ method. The specific primers used were listed in Table 1.

2.4. Peptide prediction and sequence analysis

Following the *Larimicin*'s amino acid sequences, the truncated peptide regions with high AMP potential were analyzed by the $CAMP_{R4}$ database (http://www.camp.bicnirrh.res.in/). The positive charge and hydrophobicity of the truncated peptide $Larimicin_{78\text{-}102}$ were analyzed using HeliQuest (https://heliquest.ipmc.cnrs.fr/cgi-bin/ComputParams.py). The secondary structure of *Larimicin* was predicted by SOPMA (https://npsa-prabi.ibcp.fr/cgi-bin/npsa_automat.pl?page=/NPSA/npsa_sopma.html). Three-dimensional structures of *Larimicin* and $Larimicin_{78\text{-}102}$ were predicted using I-TASSER and Alphafold, respectively.

2.5. Peptide synthesis

The truncated peptide $Larimicin_{78\text{-}102}$ (RMRRLTVWFTSPLNTA RLLNNSEVR) derived from Larimicin was synthesized using solid-phase chemistry by GenScript (Nanjing, China). Its purity was assessed to be greater than 95 % using reverse-phase high-performance liquid chromatography (RP-HPLC), and the molecular weight was measured by electrospray ionization mass spectrometry (ESI-MS). The peptide was stored as white lyophilized powder at −80 °C.

2.6. Antimicrobial assay

The minimum inhibitory concentrations (MICs), minimum bactericidal concentrations (MBCs) and minimum fungicidal concentrations (MFCs) of $Larimicin_{78\text{-}102}$ were assessed using the broth dilution method [27]. Briefly, bacteria in the exponentially phase were collected and diluted with Muller-Hinton broth (MH) (HKM, China). *Vibrio* species were diluted in tryptic soy broth (TSB) (Hopebio, China) supplemented with 2 % NaCl to approximately 10^5 CFU/mL. Logarithmic phase fungi were diluted to approximately 2×10^4 cells/mL with RPMI-MOPS (pH 7.0) [28]. $Larimicin_{78\text{-}102}$ was diluted with Milli-Q water in a gradient (3–96 μM). Then, equal volumes of bacteria and $Larimicin_{78\text{-}102}$ were incubated at 37 °C or 28 °C for 24 h. After 24 h of incubation, MIC, MBC and MFC values were determined. The MIC is defined as the lowest peptide concentration at which no visible bacterial growth is observed, while the MBC refers to the lowest peptide concentration required to kill 99.9 % of bacteria, and the MFC represents the minimum peptide concentration that kills 99.9 % of fungi. The experiments were conducted in triplicate, and each was repeated three times.

2.7. Time-killing kinetics

The time-killing kinetics assay was used to assess the bactericidal effect of $Larimicin_{78\text{-}102}$ against *V. fluvialis*, *P. fluorescens* and *P. putida* [28]. Briefly, the bacteria were collected and diluted to 10^5 CFU/mL, and co-incubated with $Larimicin_{78\text{-}102}$ at a final concentration of 12 μM (1 × MBC). *V. fluvialis* mixtures were diluted and plated on 2216 E agar at different time point. The diluted suspensions of *P. fluorescens* and *P. putida* were inoculated onto nutrient broth (NB) agar at distinct time points. These plates were incubated at 28 °C for 24 h. The colonies were counted. The experiments were conducted three times, each in triplicate.

2.8. Biofilm inhibition assay

The formation capability of biofilm was determined through the crystal violet (CV) method [29]. Bacteria in the exponentially growth phase were harvested and adjusted to 10^5 CFU/mL (*V. fluvialis*) in TSB

supplemented with 2 % NaCl, and to 10^7 CFU/mL (*P. fluorescens* and *P. putida*) in MH broth. A series of Larimicin$_{78\text{-}102}$ concentrations (0, 3, 6, 12, 24, 48, and 96 μM) were co-incubated with equal amounts of bacteria at 28 °C for 16 h (*V. fluvialis*) or 24 h (*P. fluorescens* and *P. putida*). Following incubation, the upper layer of planktonic cells was discarded and the wells underwent three washes with PBS. The cell-plates were placed at 65 °C for 30 min. Crystal violet (0.1 %, w/v) was added to the plates and incubated for 15 min under room temperature conditions. The wells were washed with Milli-Q water until there was no obvious color. The readings at 595 nm were measured using a microplate reader (Tecan, Switzerland). The experiments were carried out three times, each with three replicates.

Eradication of preformed biofilms was evaluated by resazurin after Larimicin$_{78\text{-}102}$ treatment. *V. fluvialis*, *P. fluorescens*, and *P. putida* were adjusted to approximately 10^5 CFU/mL. They were placed in 96-well plates and incubated for 16 h (*V. fluvialis*) or 24 h (*P. fluorescens* and *P. putida*). Then, the supernatant was eliminated and subjected to three washes with PBS. Subsequently, different concentrations of Larimicin$_{78\text{-}102}$ (1.5, 3, 6, 12, 24, and 48 μM) together with resazurin (final concentration of 0.1 mM) were introduced. Incubation was continued for 6 h. Absorbance readings were recorded at 560 nm and 620 nm using a microplate reader (Tecan, Switzerland). The experiments were carried out three times, each with three replicates.

2.9. SEM and TEM observation

The morphological changes of *V. fluvialis*, *P. fluorescens*, and *P. putida* were visualized by scanning electron microscope (SEM), following the previously established methods [30]. Briefly, *V. fluvialis*, *P. fluorescens*, and *P. putida* in the exponential phase were diluted to about 10^7 CFU/mL and co-incubated with Larimicin$_{78\text{-}102}$ at a final concentration of 12 μM or 24 μM (1 × MBC or 2 × MBC). The incubation of *V. fluvialis* cultures was performed at 28 °C for 120 min, while *P. fluorescens* and *P. putida* mixtures were kept for 90 min at the same temperature. Following incubation, the bacterial mixtures were centrifuged at 6000 g for 5 min, washed three times with PBS, and fixed overnight at 4 °C with an equal volume of 2.5 % glutaraldehyde. After discarding the supernatant, the samples underwent three washes with PBS before being mounted on glass slides. Subsequently, dehydration of the cells was performed using ethanol at concentrations ranging from 30 % to 100 %. The samples were dried by a critical point dryer (EM CPD300, Leica, Germany) and sprayed with gold. Finally, the morphological changes of the samples were examined using SEM (FEI Quanta 650 FEG, Thermo Fisher, USA).

Transmission electron microscope (TEM) experiment was performed on a previous basis with some adjustments [30]. Larimicin$_{78\text{-}102}$ (final concentration of 24 μM, 2 × MBC) was co-incubated with approximately 10^8 CFU/mL bacteria. The incubation of *V. fluvialis* or *P. putida* mixtures lasted 30 min at 28 °C, and *P. fluorescens* mixtures were maintained for 90 min at the same temperature. The samples were treated following the same procedure as mentioned earlier for SEM analysis. Next, the samples were washed three times with PBS, added to the agar model and fixed again overnight at 4 °C. The samples were rinsed with PBS, and dehydrated through an ethanol gradient, and then embedded in epoxy resin. Sections were prepared using an ultramicrotome, followed by TEM imaging (HT-7800, Hitachi, Japan).

2.10. Lipopolysaccharides binding assay

The concentrations of *V. fluvialis*, *P. fluorescens*, and *P. putida* were adjusted according to the antimicrobial assays. Larimicin$_{78\text{-}102}$ at a final concentration of 12 μM (1 × MBC, 25 μL) and lipopolysaccharides (LPS) (0, 4, 8, 16, and 32 μg/mL, 25 μL) were added to 96-well plates. Then, 50 μL of bacteria were added to 96-well plates. Measurements of absorbance at 600 nm were conducted every 12 h using a microplate reader (Tecan, Switzerland). Three independent experiments were performed, each including three parallel tests.

2.11. NPN uptake assay

To analyze outer membrane's permeability, we employed the uptake assay using N-phenyl-1-naphthylamine (NPN) (Sigma-Aldrich, USA) following the method previously outlined [31]. Bacteria in the log-phase of growth were harvested and diluted with HEPES buffer containing 5 mM HEPES and 5 mM glucose (pH 7.4), adjusting the concentration to 10^7 CFU/mL. NPN was diluted in 95 % ethanol and mixed with the bacterial suspension to a final concentration of 10 μM, followed by a 15 min incubation. Fluorescence measurements were taken at 350 nm excitation and 420 nm emission. After detection of background values, different concentrations of Larimicin$_{78\text{-}102}$ (0, 3, 6, 12, 24, and 48 μM) or polymyxin B (PMB, 2 μg/mL) were dispensed into every well. The effect of Larimicin$_{78\text{-}102}$ on NPN uptake was examined every 2 min. Three independent experiments were performed, each including three parallel tests.

2.12. SYTOX green uptake assay

SYTOX Green exhibits fluorescence by binding to DNA. With minor adjustments to the previously methods, the SYTOX Green uptake assay was conducted [32]. Logarithmic phase bacteria were harvested and adjusted to a concentration of 10^7 CFU/mL. The bacteria and SYTOX Green (at a final concentration of 2.5 μM) were incubated for 15 min. Subsequently, final concentrations of Larimicin$_{78\text{-}102}$ (3, 6, 12, 24, and 48 μM) were added to the mixture. The microplate reader (excitation at 485 nm, emission at 520 nm) (Tecan, Switzerland) was used to measure fluorescence intensity every 5 min. Three independent experiments were performed, each including three parallel tests.

2.13. Live/dead staining assay

The extent of membrane damage was detected using the LIVE/DEAD BacLight™ Bacterial Viability Kit (Thermo Fisher, USA). *V. fluvialis*, *P. fluorescens*, and *P. putida* were diluted to 10^7 CFU/mL with culture medium. Then, different concentrations of Larimicin$_{78\text{-}102}$ (final concentrations of 12 and 24 μM) were mixed into the bacterial suspension. 2 μg/mL PMB acted as a positive control. The samples were resuspended in a SYTO9/PI dye mixture after incubation and examined with a confocal laser scanning microscope (CLSM) (Zeiss LSM780, Germany).

2.14. ATP release

V. fluvialis, *P. fluorescens*, and *P. putida* were adjusted to about 10^7 CFU/mL in PBS. Larimicin$_{78\text{-}102}$ was mixed with the bacterial suspension to achieve 3, 6, 12, 24, and 48 μM final concentrations. 1 % Triton X-100 and PMB (2 μg/mL) were used as positive controls. The mixtures were incubated at 28 °C for 20 min. The extracellular ATP levels of the supernatant were analyzed in accordance with the guidelines of the Enhanced ATP Assay Kit (Beyotime, China). The experiments were conducted three times, each in triplicate.

2.15. ROS measurement

The fluorescent probe DCFH-DA (Nanjing, China) was used to evaluate reactive oxygen species (ROS) levels. These bacteria were diluted in PBS to roughly 10^7 CFU/mL, followed by the addition of 10 μM DCFH-DA to the suspension. Subsequently, final concentrations of Larimicin$_{78\text{-}102}$ (3, 6, 12, 24, and 48 μM) were transferred to the mixture and incubated in the dark for 15 min. The fluorescence was detected using a microplate reader (Tecan, Switzerland) at 488 nm excitation and 525 nm emission. Three independent experiments were performed, each including three parallel tests.

A

```
1                                                ACATGGGGATTCACATATCAGCTCTTCAACAGCAA
61    CTTGAGGCTCAGGTGTGTATGCTGTAACAATATGCTACCTGAGACTCTCCTCCAGCAGTG
96    ATGCCTGCCTTCAGCCCTCCTGCCTCTTTCCTCTGCGTGCTGCTGTGTGTGTCTGTAGCT
1     M  P  A  F  S  P  P  A  S  F  L  C  V  L  L  C  V  S  V  A
156   CTGCAGCGCTCTGACCTGCGCCTGGCTTATGTGACCCACAACAGCTTTTTCTACTACTCC
21    L  Q  R  S  D  L  R  L  A  Y  V  T  H  N  S  F  F  Y  Y  S
216   TGCAGCCAGGACCCGCAACCCTGCAGCGTTGCCTCACTTGCAGACTGCAGATGCAAGGAC
41    C  S  Q  D  P  Q  P  C  S  V  A  S  L  A  D  C  R  C  K  D
276   ATCCAGCTTTCCACGCTGCACCGTCCCCAGTCTCACTCGTCTCCTGTTTTCCGGATGAGA
61    I  Q  L  S  T  L  H  R  P  Q  S  H  S  S  P  V  F  R  M  R
336   CGTTTAACCGTTTGGTTCACGTCGCCGTTAAACACAGCACGTCTGCTCAATAACTCAGAG
81    R  L  T  V  W  F  T  S  P  L  N  T  A  R  L  L  N  N  S  E
396   GTAAGACACCTCACCCTCATCCACTGTGGTGCTGGAGGATCCAGAGGGACACCTTCTTCT
101   V  R  H  L  T  L  I  H  C  G  A  G  G  S  R  G  T  P  S  S
456   TCCTTGGAGGGACATTTTGCTGTGCAGCACCTCGAGAGGCTGACGGTGGTGAACCTACCG
121   S  L  E  G  H  F  A  V  Q  H  L  E  R  L  T  V  V  N  L  P
516   CAGAGGCCGGTTCCCCAATGTCCAGATGGAAGCAAAGCCAAAAACACAGACTCAAACATT
141   Q  R  P  V  P  Q  C  P  D  G  S  K  A  K  N  T  D  S  N  I
576   GACCCAGACAGAGATAATGCTGCTCATGTAGACAGAAATAGATACAACAAGGATAGAGGC
161   D  P  D  R  D  N  A  A  H  V  D  R  N  R  Y  N  K  D  R  G
636   TCAAACCTGGACCTGATTGTGGACATGAAGAAAGATTCCTCAGCTTTGCCCTCACCTCAG
181   S  N  L  D  L  I  V  D  M  K  K  D  S  S  A  L  P  S  P  Q
696   ATCCAAGACATCTTACTGGGCAGGGAGCTGGGAGCAGCGTATCACGAACAGGCCAGACTG
201   I  Q  D  I  L  L  G  R  E  L  G  A  A  Y  H  E  Q  A  R  L
756   GGAATCATCCACAGCTCTGTGCTGGAGTGGGGAGCAGTGGTCAAAGCGTACACAGTCCAG
221   G  I  I  H  S  S  V  L  E  W  G  A  V  V  K  A  Y  T  V  Q
816   ACACACATAGACAATGACGGCATGCTGCCCTTCCCTGACCTCCACCTGCCAAAATTACCA
241   T  H  I  D  N  D  G  M  L  P  F  P  D  L  H  L  P  K  L  P
876   GAGACGTCTGTGATATATGTCAGCTTTGTTTACTGA
261   E  T  S  V  I  Y  V  S  F  V  Y  *
912   TACCAGACAGTGTTCACGACCTGCAAACAATCACTTTTTTTGTTACTTTGGGCATAAGAA
972   TATGATAAGAAATAGGGGATAAAGTGGTCATCAGTTTACAGAATATGTTGCATTTAACGT
1032  TAGAGATGAACTTAAAGAAACTCTTAAATGACCAAAAACTGATAACAAACATATTTTGTT
1092  CTGCCAGTTTTAGATTTTCTCAGTTTTTTGAGAAGAAAATAGTTTGTTTGTTTACTCCAA
1152  AGTTAAAGCACATTTTTTGGCACAAATGCACAAACACACACAAAATACGTGAAAACCTGA
1212  AATTTTGCACAGCTGTTTATCAGCATGTTAGAACG
```

B

C

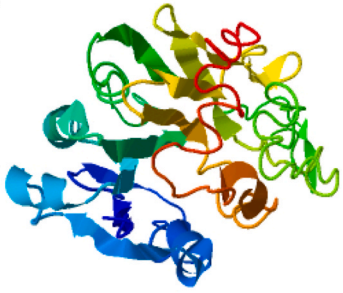

D

Physicochemical parameters	Larimicin$_{78\text{-}102}$
Sequence	RMRRLTVWFTSPLNTARLLNNSEVR
Number of amino acids	25
Molecular formula	$C_{132}H_{220}N_{44}O_{36}S_1$
Molecular weight	3031.53 Da
Total net charge	+4
Theoretical Isoelectric point	12.18
Hydrophobicity	35%

E

Fig. 1. Sequence analysis of the *Larimicin* and Larimicin$_{78\text{-}102}$. (A) Full-length cDNA and amino acid sequences of *Larimicin*. The green underline represents the signal peptide. The red underline represents the predicted truncated peptide. (B) Prediction of secondary structure of *Larimicin* by SOPMA. (C) Prediction of tertiary structure of *Larimicin* by I-TASSER. (D) The amino acid sequence and key physicochemical parameters of Larimicin$_{78\text{-}102}$. (E) The predicted tertiary structure of Larimicin$_{78\text{-}102}$ using the AlphaFold. (For interpretation of the references to color in this figure legend, the reader is referred to the Web version of this article.)

2.16. Thermal stability and cation tolerance assay

A 24 μM concentration of Larimicin$_{78\text{-}102}$ was incubated at different temperatures (40, 60, 80, 100 °C) for 30 min. *V. fluvialis*, *P. fluorescens*, and *P. putida* were diluted to approximately 10^5 CFU/mL and then mixed with Larimicin$_{78\text{-}102}$. The readings were performed at 600 nm every 12 h by a microplate reader (Tecan, Switzerland). Three independent experiments were performed, each including three parallel tests.

For the cation tolerance assay, the bacterial concentration was the same as the above assay. The prepared bacterial suspensions were mixed with Larimicin$_{78\text{-}102}$ at a final concentration of 12 μM, followed by the

addition of NaCl solutions at concentrations of 10, 20, 40, 80, and 160 mM. Absorbance was assessed at 600 nm every 12 h with a microplate reader (Tecan, Switzerland). Three independent experiments were performed, each including three parallel tests.

2.17. Cytotoxicity and hemolytic activity

The cytotoxicity of Larimicin$_{78\text{-}102}$ on cell lines (HEK-293T, RAW264.7, ZF4 and LYCK) was examined using the MTS-PMS assay. These cells were adjusted to a concentration of 1×10^5 cells/mL. Then, the cell suspension was placed into 96-well plates (100 μL/well) and cultured overnight. After the supernatant was removed, fresh medium containing different concentrations of Larimicin$_{78\text{-}102}$ (1.5, 3, 6, 12, 24, and 48 μM) was added and incubated overnight. The cell viability was evaluated at 492 nm using a microplate reader (Tecan, Switzerland). Three independent experiments were performed, each including three parallel tests.

Hemolytic activity of Larimicin$_{78\text{-}102}$ on mouse erythrocytes was determined as previously mentioned [33]. Briefly, mouse erythrocytes were acquired and diluted to 4 % erythrocytes using 0.9 % saline. Equal volumes of erythrocytes were incubated with various concentrations of Larimicin$_{78\text{-}102}$ (1.5, 3, 6, 12, 24, and 48 μM) for 1 h at 37 °C. Saline served as the negative control, while 1 % Triton X-100 acted as the positive control. After centrifugation at 4000*g* for 3 min, the clear supernatant was transferred to a fresh 96-well plate. The readings at 540 nm were documented with a microplate reader (Tecan, Switzerland). Three independent experiments were performed, each including three parallel tests.

2.18. Animal assay

To reveal the anti-infective effect of Larimicin$_{78\text{-}102}$ *in vivo*, an animal model of *V. fluvialis* infection was established in large yellow croaker. Large yellow croaker was intraperitoneally infected with *V. fluvialis* at different concentrations of 8×10^5 CFU/100 μL, 4×10^6 CFU/100 μL, 2×10^7 CFU/100 μL, 1×10^8 CFU/100 μL, and 5×10^8 CFU/100 μL. PBS was used as the control group. The survival rate of the fish was recorded. The LC_{50} of *V. fluvialis* infection in large yellow croaker at 168 h was analyzed using the Probit method.

Healthy fish (30 ± 10 g, n = 60) were randomly divided into three groups: the PBS control group, the *V. fluvialis* infection group, and the Larimicin$_{78\text{-}102}$ treatment group, with 20 fish in each group. Fish were intraperitoneally injected with *V. fluvialis* (4.34×10^8 CFU/mL) for 1 h prior to the injection of PBS or Larimicin$_{78\text{-}102}$ (10 μg/fish). The surviving fish were counted at different time point, and the survival curves were plotted using GraphPad Prism 8.0. The independent experiments were performed at least twice.

The fish tissues (intestine and spleen, n = 3) were gathered and maintained at −80 °C for RNA extraction. The expression levels of three inflammatory cytokines (*TNF-α*, *IL-1β* and *IL-4*) and three AMP genes (*piscidin*, *hepcidin*, and *lysozyme*) were analyzed by qPCR. The enzymatic activity of lysozyme in the intestine and spleen was quantified using the LZM assay kit (Nanjing, China).

2.19. Statistical analysis

All results were provided as mean ± standard deviation (SD). Statistical analyses were conducted with GraphPad Prism 8.0 and SPSS 22.0 software. The differential expression analysis of Figs. 2 and 9 was conducted using Student's *t*-test. One-way ANOVA was used to analyze the variations in bacterial biofilm clearance of Fig. 3, ATP levels and ROS production of Fig. 7. A significance level of 95 % ($p < 0.05$) was set for differences among groups.

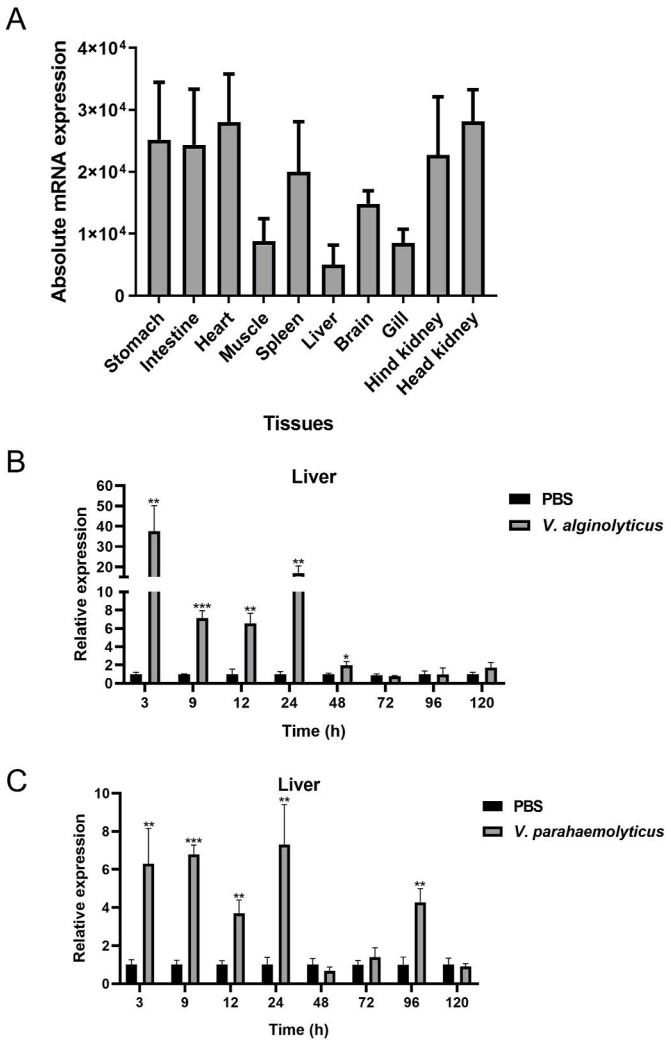

Fig. 2. Gene expression patterns of *Larimicin* in large yellow croaker. (A) Tissue distribution of *Larimicin* in healthy large yellow croaker. The relative expression of *Larimicin* in the liver after *V. alginolyticus* (B) or *V. parahaemolyticus* (C) challenge. Statistical significance is indicated by asterisks, $*p < 0.05$, $**p < 0.01$ and $***p < 0.001$.

3. Results

3.1. Cloning and sequence analysis of Larimicin

The full-length cDNA sequence of *Larimicin* is 1246 bp (GenBank accession number OR161972), with an open reading frame of 816 bp, a 5′ untranslated region (UTR) of 95 bp containing cap sequences and a 3′ UTR of 335 bp containing poly(A) tail (Fig. 1A). Blast alignment of the amino acid sequence of Larimicin revealed that this protein is uncharacterized through NCBI Blast. The top 10 alignment results are listed in Table 2. The cleavage position of *Larimicin* was between Gln-22 and Arg-23. The mature peptide consists of 249 amino acids, with a molecular mass of 27.825 kDa and a theoretical isoelectric point (pI) of 7.83. Predictions of secondary and tertiary structures revealed that *Larimicin* contains eight α-helices and ten β-sheets (Fig. 1B and C).

The truncated peptide of *Larimicin* (located at 78th to 102nd) was designed using the CAMP$_{R4}$ database. The key physicochemical parameters of Larimicin$_{78\text{-}102}$ were shown in Fig. 1D. The predicted molecular weight and pI were 3.031 kDa and 12.18, respectively. Larimicin$_{78\text{-}102}$ had a total net charge of +4 and a hydrophobicity of 35 %. The predicted tertiary structure of Larimicin$_{78\text{-}102}$ consists mainly of an α-helix (Fig. 1E).

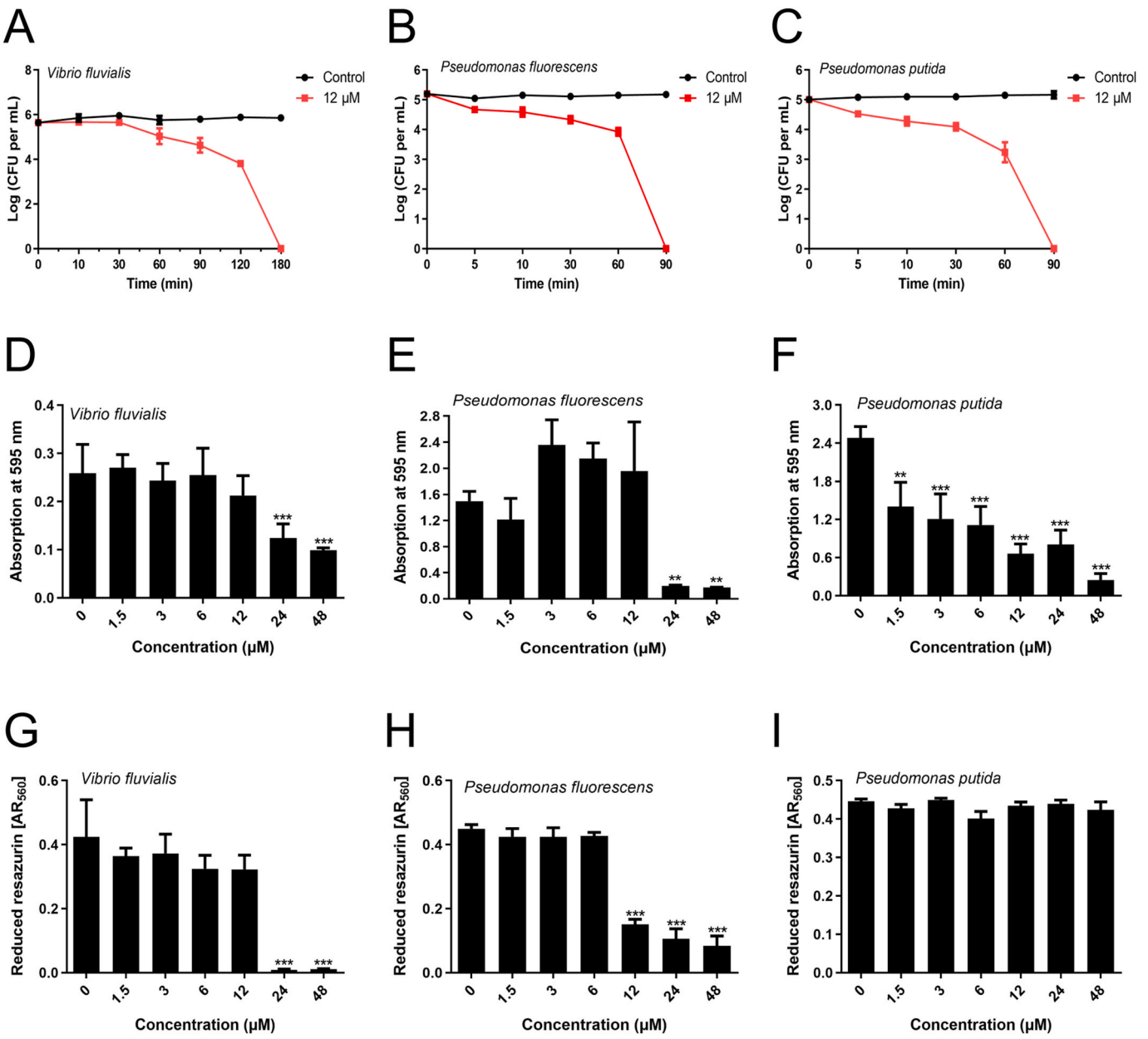

Fig. 3. Time-killing kinetic curves of Larimicin$_{78\text{-}102}$ on *V. fluvialis* (A), *P. fluorescens* (B) and *P. putida* (C). The inhibitory effects of Larimicin$_{78\text{-}102}$ on *V. fluvialis* (D), *P. fluorescens* (E) and *P. putida* (F) biofilm formation, or *V. fluvialis* (G), *P. fluorescens* (H) and *P. putida* (I) mature biofilm. Statistical significance is indicated by asterisks, $^{*}p < 0.05$, $^{**}p < 0.01$ and $^{***}p < 0.001$.

3.2. Expression profiles of Larimicin

The *Larimicin* gene expression in various tissues of healthy large yellow croaker was determined. *Larimicin* was found to be extensively present in all examined tissues (Fig. 2A). The LC_{50} of *V. alginolyticus* (1.72×10^7 CFU/100 μL) or *V. parahaemolyticus* (6.5×10^7 CFU/100 μL) was obtained using Probit analysis (Supplementary Fig. 1). To clarify the role of *Larimicin* in the immune response, the mRNA expression of *Larimicin* was analyzed in the liver after *V. alginolyticus* or *V. parahaemolyticus* challenge. The results revealed that *Larimicin* expression was significantly up-regulated at 3, 9, 12, 24, and 48 h in the liver after *V. alginolyticus* infection (Fig. 2B). Similarly, this gene was markedly up-regulated at 3, 9, 12, 24, and 96 h after *V. parahaemolyticus* stimulation (Fig. 2C).

3.3. Antimicrobial activity of Larimicin$_{78\text{-}102}$

The antimicrobial activity of Larimicin$_{78\text{-}102}$ was measured against a series of strains and expressed as MIC, MBC and MFC. As shown in Table 3, Larimicin$_{78\text{-}102}$ manifested a broad-spectrum antimicrobial activity against Gram-positive bacteria (*S. aureus*, *S. epidermidis*), Gram-negative bacteria (*A. baumannii*, *P. putida*, *P. aeruginosa*, *P. fluorescens*, *P. stutzeri*, *S. flexneri*, *E. coli*, *V. fluvialis*, *V. alginolyticus*, *V. parahaemolyticus*), and fungi (*C. neoformans*) with MIC values ranging from 3 μM to 48 μM, and MBC or MFC values below 48 μM.

3.4. Killing kinetic

The bactericidal efficiency of Larimicin$_{78\text{-}102}$ was assessed by a time-killing kinetic assay. Larimicin$_{78\text{-}102}$ killed *V. fluvialis*, *P. fluorescens*, and *P. putida* in a time-dependent manner (Fig. 3A–C). Larimicin$_{78\text{-}102}$ killed

Table 2
Amino acid sequence alignment of Larimicin with other protein.

Species name	GenBank	Protein name	Amino acid identity (%)
Larimichthys crocea	OR161972	Larimicin	–
Collichthys lucidus	TKS85808.1	Hypothetical protein	98.52
Centropristis striata	XP_059215708.1	Uncharacterized protein	88.93
Chelmon rostratus	XP_041803906.1	Uncharacterized protein	88.56
Toxotes jaculatrix	XP_040905543.1	Uncharacterized protein	88.19
Mastacembelus armatus	XP_026165966.1	Uncharacterized protein	87.08
Lates japonicus	GAA6231609.1	Uncharacterized protein	87.00
Siniperca chuatsi	XP_044071022.1	Uncharacterized protein	86.72
Morone saxatilis	XP_035520073.1	Uncharacterized protein	86.35
Scortum barcoo	KAI3362747.1	Uncharacterized protein	85.71
Plectropomus leopardus	XP_042358502.1	Uncharacterized protein	85.61

Table 3
Antimicrobial activity of Larimicin$_{78\text{-}102}$.

Microorganism	CGMCC No.[a]	MIC (μM)[b]	MBC/MFC (μM)[c]
Gram-positive bacteria			
Staphylococcus aureus	1.2465	12–24	24–48
Staphylococcus epidermidis	1.4260	12–24	12–24
Gram-negative bacteria			
Acinetobacter baumannii	1.6769	6–12	12–24
Pseudomonas stutzeri	1.1803	1.5–3	6–12
Shigella flexneri	1.1868	6–12	12–24
Pseudomonas aeruginosa	1.2421	24–48	24–48
Escherichia coli	1.2389	12–24	12–24
Pseudomonas putida	1.3136	6–12	6–12
Pseudomonas fluorescens	1.3202	6–12	6–12
Vibrio fluvialis	1.1609	6–12	6–12
Vibrio alginolyticus	1.1833	12–24	12–24
Vibrio parahaemolyticus	1.1997	24–48	24–48
Fungi			
Cryptococcus neoformans	2.1563	6–12	6–12

[bc] The value of MIC and MBC/MFC are expressed as intervals [a]-[b]. [a] is the highest concentration of visible microorganisms, [b] is the lowest concentration of invisible microorganisms.
[a] China General Microbiological Culture Collection Center.

99.9 % of *V. fluvialis* in 180 min (Fig. 3A). And Larimicin$_{78\text{-}102}$ killed 99.9 % of *P. fluorescens* and *P. putida* within 90 min (Fig. 3B and C).

3.5. Anti-biofilm activity of Larimicin$_{78\text{-}102}$

The inhibitory effect of Larimicin$_{78\text{-}102}$ on the biofilm formation of *V. fluvialis*, *P. fluorescens*, and *P. putida* was evaluated. A 24 μM concentration of Larimicin$_{78\text{-}102}$ significantly impaired the ability of *V. fluvialis* and *P. fluorescens* to form biofilms (Fig. 3D and E). When the concentration of Larimicin$_{78\text{-}102}$ reached 1.5 μM, the biofilm formation of *P. putida* was significantly inhibited (Fig. 3F).

Furthermore, the inhibitory activity of Larimicin$_{78\text{-}102}$ against mature biofilms was evaluated with resazurin (Fig. 3G–I). The concentrations of Larimicin$_{78\text{-}102}$ required to inhibit *V. fluvialis* and *P. fluorescens* mature biofilms were 24 μM and 12 μM, respectively (Fig. 3G and H). Whereas Larimicin$_{78\text{-}102}$ failed to inhibit the mature biofilm of *P. putida* (Fig. 3I).

3.6. Morphological changes of microorganism

The morphological changes of bacteria were observed after Larimicin$_{78\text{-}102}$ treatment by SEM. The bacteria in the control group exhibited intact and smooth surfaces. However, the bacterial cell membrane was roughened and shriveled, with disruption of membrane integrity and leakage of cytoplasm after Larimicin$_{78\text{-}102}$ treatment. As the concentration increased, the cells lost their original morphology and fragmented (Fig. 4A). TEM was used to further observe the morphological and structural changes in the bacteria. As shown in Fig. 4B, V *fluvialis*, *P. fluorescens* and *P. putida* in the control group had dense cytoplasm, intact membrane structure and smooth surface. After exposure to 24 μM of Larimicin$_{78\text{-}102}$, the cell exhibited low electron density, cellular cavitation, fragmentation of the cell membrane, and leakage of intracellular contents. These results suggested that Larimicin$_{78\text{-}102}$ can increase bacterial membrane permeability, leading to membrane disruption and cytoplasmic leakage.

3.7. LPS reduced the efficacy of Larimicin$_{78\text{-}102}$

We investigated whether Larimicin$_{78\text{-}102}$ interacts with LPS on the outer membrane of Gram-negative bacteria to further disrupt the cell membrane. Larimicin$_{78\text{-}102}$ maintained its antimicrobial activity against *V. fluvialis* and *P. fluorescens* within 12 h after the addition of 16 μg/mL LPS to the mixture (Fig. 5A and B). However, its inhibitory effect on *V. fluvialis*, *P. fluorescens*, and *P. putida* was lost when 32 μg/mL LPS was added (Fig. 5A–C).

3.8. Membrane permeability of Larimicin$_{78\text{-}102}$

NPN uptake is a marker of outer membrane permeability. The fluorescence intensity of NPN is weak in an aqueous environment, but NPN is taken up by hydrophobic structures such as the phospholipid bilayer, which enhances the fluorescence intensity [34]. Larimicin$_{78\text{-}102}$ substantially elevated NPN fluorescence intensity in *V. fluvialis*, *P. fluorescens*, and *P. putida* in a dose-dependent manner (Fig. 5D–F). Moreover, SYTOX Green uptake assay was used to observe the permeability of the inner membrane. As shown in Fig. 6A–C, SYTOX Green fluorescence intensity of *V. fluvialis*, *P. fluorescens*, and *P. putida* was markedly enhanced in a concentration-dependent manner after Larimicin$_{78\text{-}102}$ treatment. SYTO9/PI was employed to examine the permeability of the bacterial inner membrane. SYTO9, a membrane penetrant dye, can enter all cells, whereas PI is capable of penetrating only cells with compromised membranes. In the control group, the entire field of view displayed green fluorescence, suggesting that the bacteria were all active. The PI-induced red fluorescence was significantly enhanced after Larimicin$_{78\text{-}102}$ or PMB treatment, further demonstrating that Larimicin$_{78\text{-}102}$ disrupted the inner membrane of *V. fluvialis*, *P. fluorescens*, and *P. putida* (Fig. 6D–F).

3.9. Effect of Larimicin$_{78\text{-}102}$ on ATP release and ROS production

Membrane permeability leads to the release of ATP, a key cellular component. As shown in Fig. 7A, the extracellular ATP level of *V. fluvialis* was significantly increased after 12 μM Larimicin$_{78\text{-}102}$ treatment. 3 μM of Larimicin$_{78\text{-}102}$ could effectively induced the release of ATP from *P. fluorescens* and *P. putida* in a concentration-dependent manner (Fig. 7B and C). Furthermore, research indicates that disruption of membrane homeostasis leads to the accumulation of ROS [35]. As shown in Fig. 7D-F, 3 μM of Larimicin$_{78\text{-}102}$ caused the accumulation of ROS in *V. fluvialis*, *P. fluorescens*, and *P. putida*.

3.10. The stability of Larimicin$_{78\text{-}102}$

The antimicrobial effectiveness of Larimicin$_{78\text{-}102}$ was evaluated under various conditions. As shown in Fig. 8A–C, Larimicin$_{78\text{-}102}$

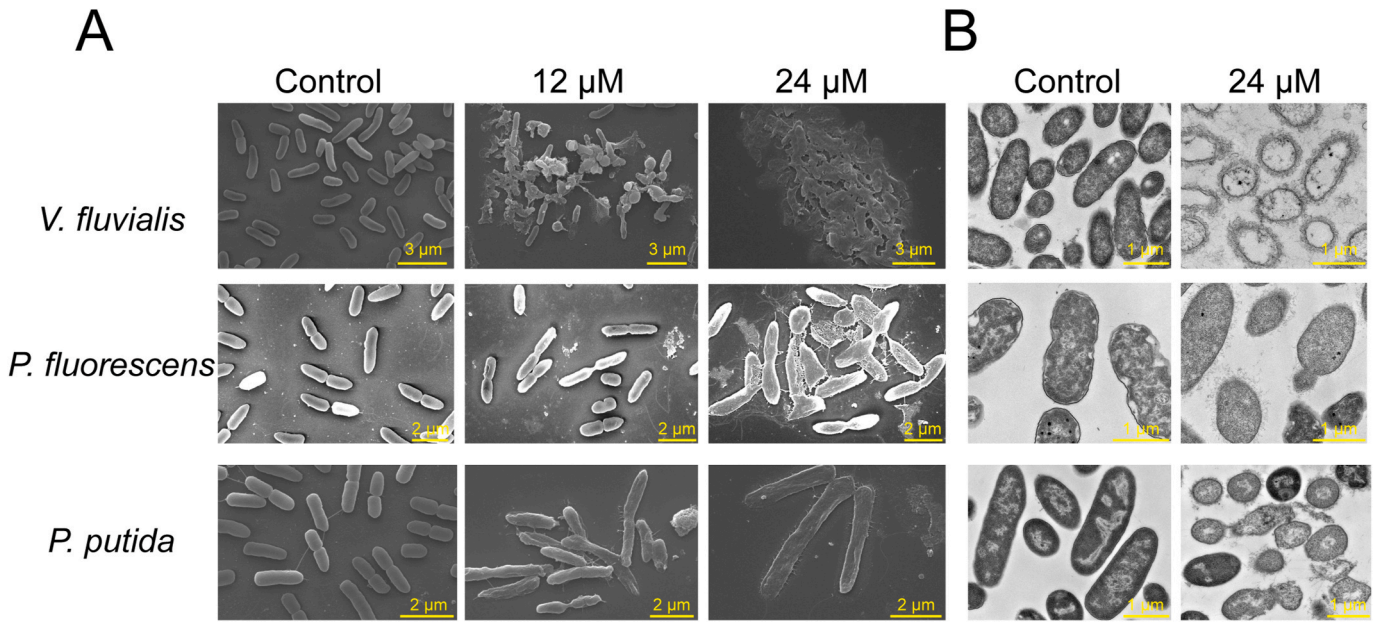

Fig. 4. Effect of Larimicin$_{78\text{-}102}$ on *V. fluvialis*, *P. fluorescens* and *P. putida* observed by SEM (A) and TEM (B).

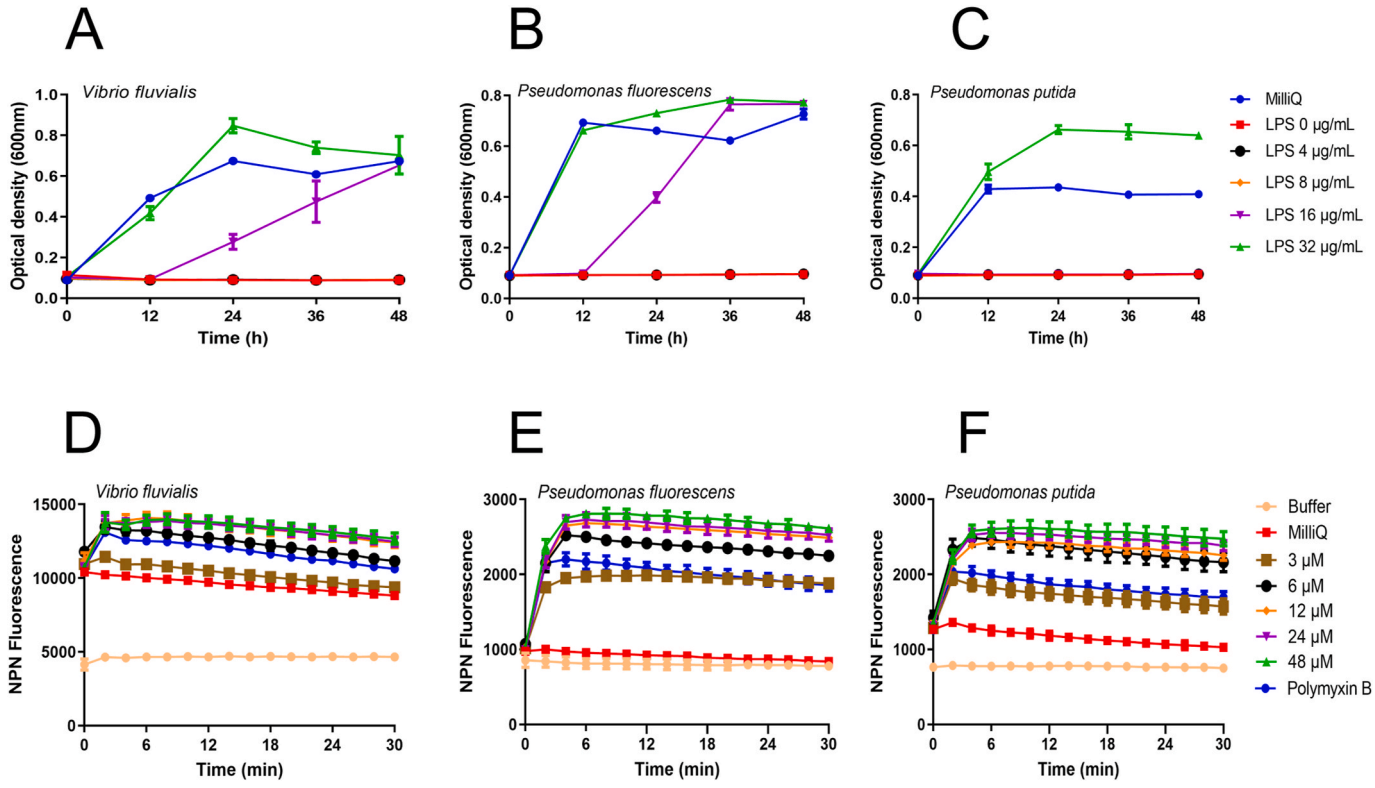

Fig. 5. Effect of exogenous LPS on Larimicin$_{78\text{-}102}$ against *V. fluvialis* (A), *P. fluorescens* (B) and *P. putida* (C). The outer membrane permeability of *V. fluvialis* (D), *P. fluorescens* (E) and *P. putida* (F) after Larimicin$_{78\text{-}102}$ treatment.

retained its sensitivity to *V. fluvialis*, *P. fluorescens*, and *P. putida* after exposure to 100 °C for 30 min, demonstrating excellent thermal stability. In addition, Larimicin$_{78\text{-}102}$ exhibited notable cation tolerance, maintaining activity against *V. fluvialis* in a 211 mM NaCl solution (Fig. 8D), and preserving efficacy against *P. fluorescens* and *P. putida* in a 160 mM NaCl (Fig. 8E and F).

3.11. Cytotoxicity and hemolytic activities of Larimicin$_{78\text{-}102}$

The cytotoxicity of Larimicin$_{78\text{-}102}$ was analyzed using HEK-293T, RAW264.7, ZF4, and LYCK cells. As shown in Fig. 8G–J, Larimicin$_{78\text{-}102}$ showed no significant cytotoxicity to these cells in the range of 1.5–48 μM. In addition, Larimicin$_{78\text{-}102}$ had no obvious hemolytic activity on mouse erythrocytes (Fig. 8K and L).

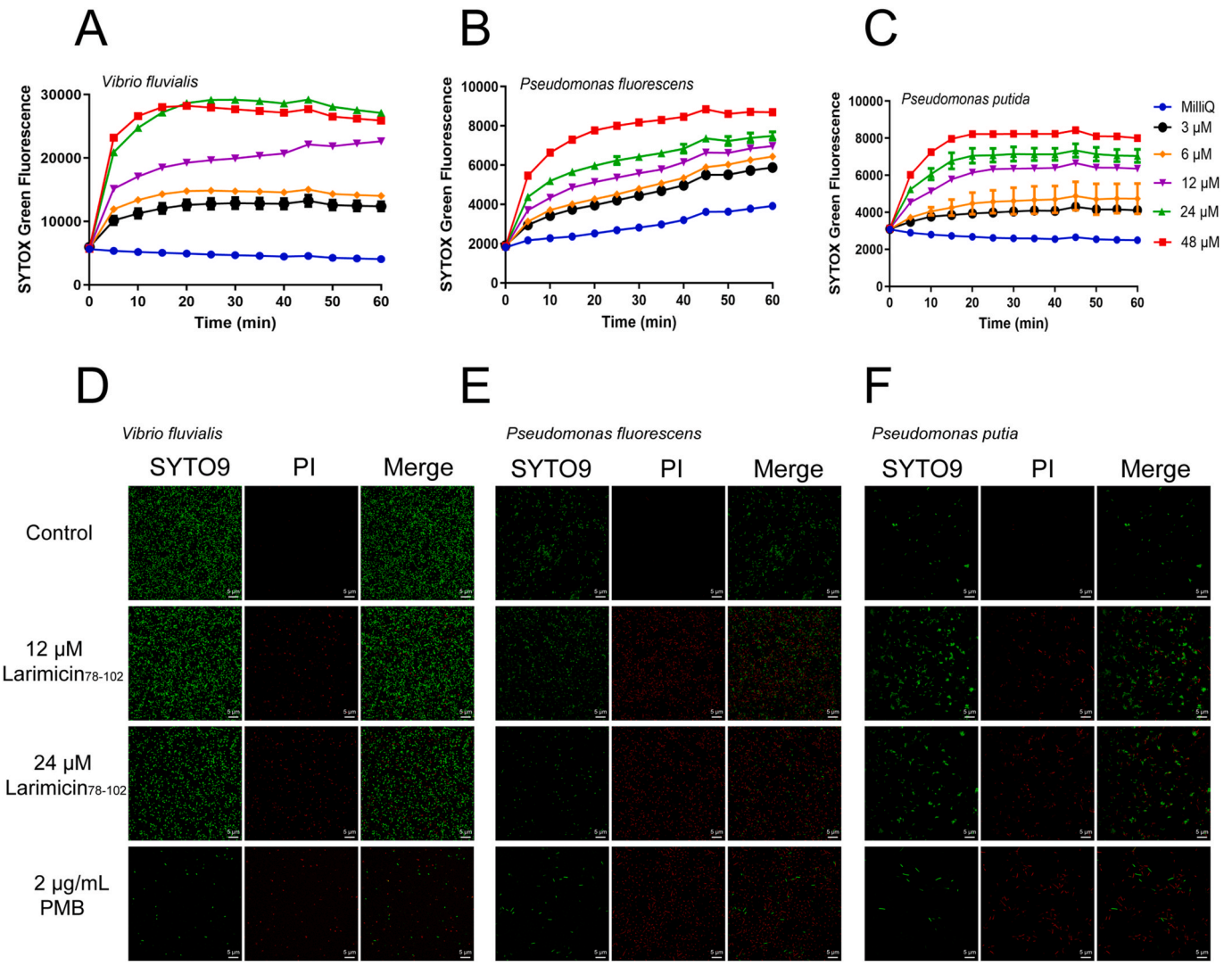

Fig. 6. Effect of Larimicin$_{78\text{-}102}$ on inner membrane permeability. SYTOX Green uptake of *V. fluvialis* (A), *P. fluorescens* (B) and *P. putida* (C) after Larimicin$_{78\text{-}102}$ treatment. The fluorescence signals of SYTO9 and PI in *V. fluvialis* (D), *P. fluorescens* (E) and *P. putida* (F). (For interpretation of the references to color in this figure legend, the reader is referred to the Web version of this article.)

3.12. *In vivo anti-V.fluvialis infection analysis*

The anti-infective effect of Larimicin$_{78\text{-}102}$ was evaluated in *L. crocea*. The 168 h LC_{50} of *V. fluvialis* infection in large yellow croaker was 4.34 $\times$ 10^8 CFU/100 μL (Supplementary Fig. 2). The schematic diagram of the *in vivo* experiment was shown in Fig. 9A. As shown in Figs. 9B, 10 μg/fish of Larimicin$_{78\text{-}102}$ effectively enhanced the survival rate of large yellow croaker after *V. fluvialis* infection. At 168 h after *V. fluvialis* infection, the survival rate in the control group dropped to 50 %, whereas the Larimicin$_{78\text{-}102}$-treated group maintained a survival rate of 95 % (Fig. 9B).

The mRNA levels of three inflammatory factors (*TNF-α*, *IL-1β*, and *IL-4*) and three AMP genes (*piscidin*, *hepcidin*, and *lysozyme*) were further examined in the intestine and spleen of large yellow croaker. As shown in Fig. 9C and D, the transcription level of the pro-inflammatory factor *IL-1β* in the intestine and spleen was markedly suppressed after treatment with Larimicin$_{78\text{-}102}$. The expression level of *TNF-α* in the intestine showed no significant difference between the *V. fluvialis* and the Larimicin$_{78\text{-}102}$ treatment group (Fig. 9C), whereas it was significantly decreased in the spleen after Larimicin$_{78\text{-}102}$ treatment (Fig. 9D). Meanwhile, the expression of the anti-inflammatory cytokine *IL-4* in the intestine and spleen was substantially increased after treatment with Larimicin$_{78\text{-}102}$ (Fig. 9C and D). Additionally, the expression levels of *piscidin*, *hepcidin*, and *lysozyme* were obviously up-regulated in the intestine after Larimicin$_{78\text{-}102}$ treatment (Fig. 9C), both *hepcidin* and *lysozyme* expression were markedly increased in the spleen (Fig. 9D). Notably, the enzymatic activity of lysozyme was significantly increased following Larimicin$_{78\text{-}102}$ treatment compared to the *V. fluvialis*-infected group (Fig. 9E and F).

4. Discussion

The intensive farming practices in aquaculture have led to the prevalence of various diseases, particularly vibriosis, a widespread bacterial disease with a high incidence rate [36]. To prevent and control bacterial infections in aquaculture, a large number of antibiotics are employed [12]. However, the emergence of antibiotic-resistant bacteria and environmental contamination in aquaculture highlights the importance of developing novel antimicrobial agents. AMPs are believed to be one of the most promising alternatives to traditional antibiotics. *L. crocea* is a crucial species in aquaculture and the most important economic fish in China and East Asia [37]. With the expansion of aquaculture, disease prevention has become critical. In our study, a novel and uncharacterized functional gene, *Larimicin*, was identified

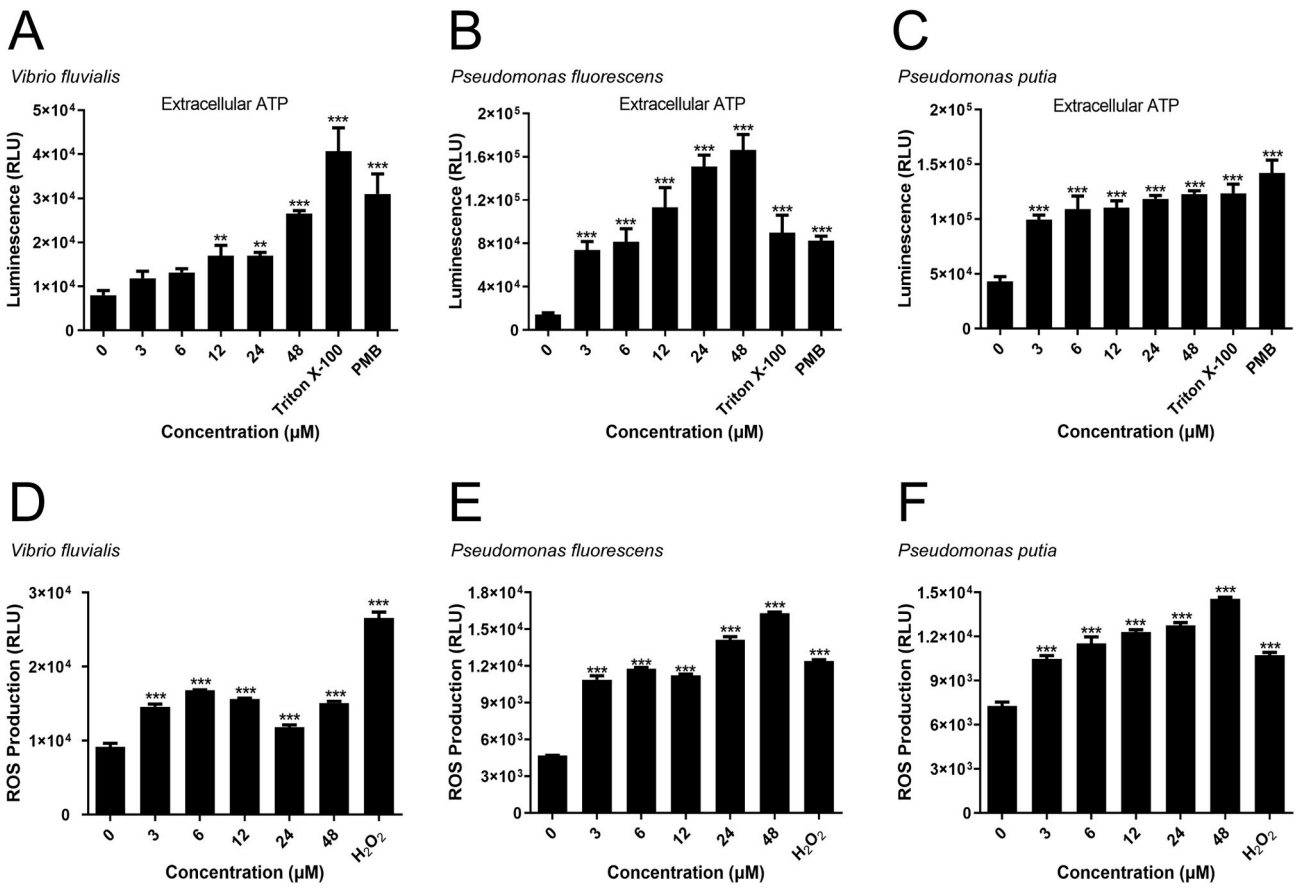

Fig. 7. ATP release of *V. fluvialis* (A), *P. fluorescens* (B) and *P. putida* (C) after Larimicin$_{78\text{-}102}$ treatment. Intracellular ROS accumulation of *V. fluvialis* (D), *P. fluorescens* (E) and *P. putida* (F) after treatment with Larimicin$_{78\text{-}102}$. Statistical significance is indicated by asterisks, $*p < 0.05$, $**p < 0.01$ and $***p < 0.001$.

from *L. crocea*. A truncated peptide, Larimicin$_{78\text{-}102}$, was screened from *Larimicin*, which exhibited broad-spectrum antimicrobial activity and effectively combated *V. fluvialis* infection, offering a promising foundation for vibriosis treatment in *L. crocea* aquaculture.

In the study, *Larimicin* was notably up-regulated in the liver with the challenge of *V. alginolyticus* and *V. parahaemolyticus*. Fish combat pathogen infections by regulating their immune system, particularly the innate immune response [38]. The main immune organs are the liver, spleen, intestine and kidney [39]. These results suggested that *Larimicin* could play a significant role in immune defense of large yellow croaker. Subsequently, Larimicin$_{78\text{-}102}$ was predicted to have potential antimicrobial activity, with a +4 net charge and 35 % hydrophobicity. In marine farming, environmental complexities can limit the efficacy of AMPs like LcCCL28-25 [40] and NK-lysin [25] against *Vibrio* infections. This study indicated that Larimicin$_{78\text{-}102}$ was highly effective *in vitro* against specific aquatic pathogens, including *V. fluvialis*, *V. parahaemolyticus*, *V. alginolyticus*, *P. putida*, and *P. fluorescens*. Moreover, the structure of Larimicin$_{78\text{-}102}$ was predicted to adopt an α-helix, which is the most common structure of AMPs and the optimal conformation for interactions with biofilms [41]. Biofilm, an extracellular polymeric substance, exhibits much greater resistance to antibiotics than planktonic cells [42,43]. Biofilms are thought to be one of the pathogenic factors contributing to *V. fluvialis* infections [44]. The discovery of anti-biofilm agents is a crucial advancement in inhibiting biofilm formation [42]. In our study, Larimicin$_{78\text{-}102}$ not only effectively inhibited the formation of *V. fluvialis* biofilm but also exhibited notable removal capabilities against mature biofilms, confirming its potential in controlling *V. fluvialis* biofilms. These results suggested that Larimicin$_{78\text{-}102}$ not only rapidly killed planktonic *V. fluvialis* but also significantly inhibited its biofilm growth.

To explore the potential of Larimicin$_{78\text{-}102}$ as a more feasible antibiotic alternative, we elucidated its antibacterial mechanisms *in vitro*. As is well known, cationic AMPs usually exert antimicrobial activity by electrostatically attaching to the negatively charged bacterial membranes [41]. We observed the effects of Larimicin$_{78\text{-}102}$ on bacterial morphology using SEM and TEM. LPS is a key component on the outer membrane of Gram-negative bacteria, and its addition significantly reduced the antibacterial activity of Larimicin$_{78\text{-}102}$, suggesting that Larimicin$_{78\text{-}102}$ may bind to bacterial outer membrane components. Subsequently, NPN uptake, SYTOX Green uptake, and SYTO9/PI assays provided additional evidence that Larimicin$_{78\text{-}102}$ enhances outer and inner membrane permeability. These results suggested that Larimicin$_{78\text{-}102}$ may act on the cell membrane of bacteria, causing membrane rupture, similar to some AMPs, such as Css54 [45] and Sp-LECin [46]. The rupture of the cell membrane may lead to the leakage of a crucial cellular component, ATP. In this study, the levels of extracellular ATP were significantly elevated after treatment with Larimicin$_{78\text{-}102}$. Thus, Larimicin$_{78\text{-}102}$ exerted antimicrobial effects by targeting and disrupting cell membranes. It is well known that membrane disruption leads to impairment of the respiratory chain and ROS accumulation [35]. ROS are commonly produced during cellular metabolism, affecting cellular signaling pathways and various physiological functions, which can result in the oxidation of DNA, proteins and lipid macromolecules, ultimately causing oxidative damage [47,48]. Several studies have found that AMPs could exert antimicrobial effects through the accumulation of ROS, such as LBLP and N1 [35,49]. In the study, Larimicin$_{78\text{-}102}$ effectively increased ROS accumulation, which could lead to cellular metabolic disorders, causing severe oxidative stress and even death. The underlying mechanisms warrant further exploration.

The activity of AMPs can be influenced by various physiological

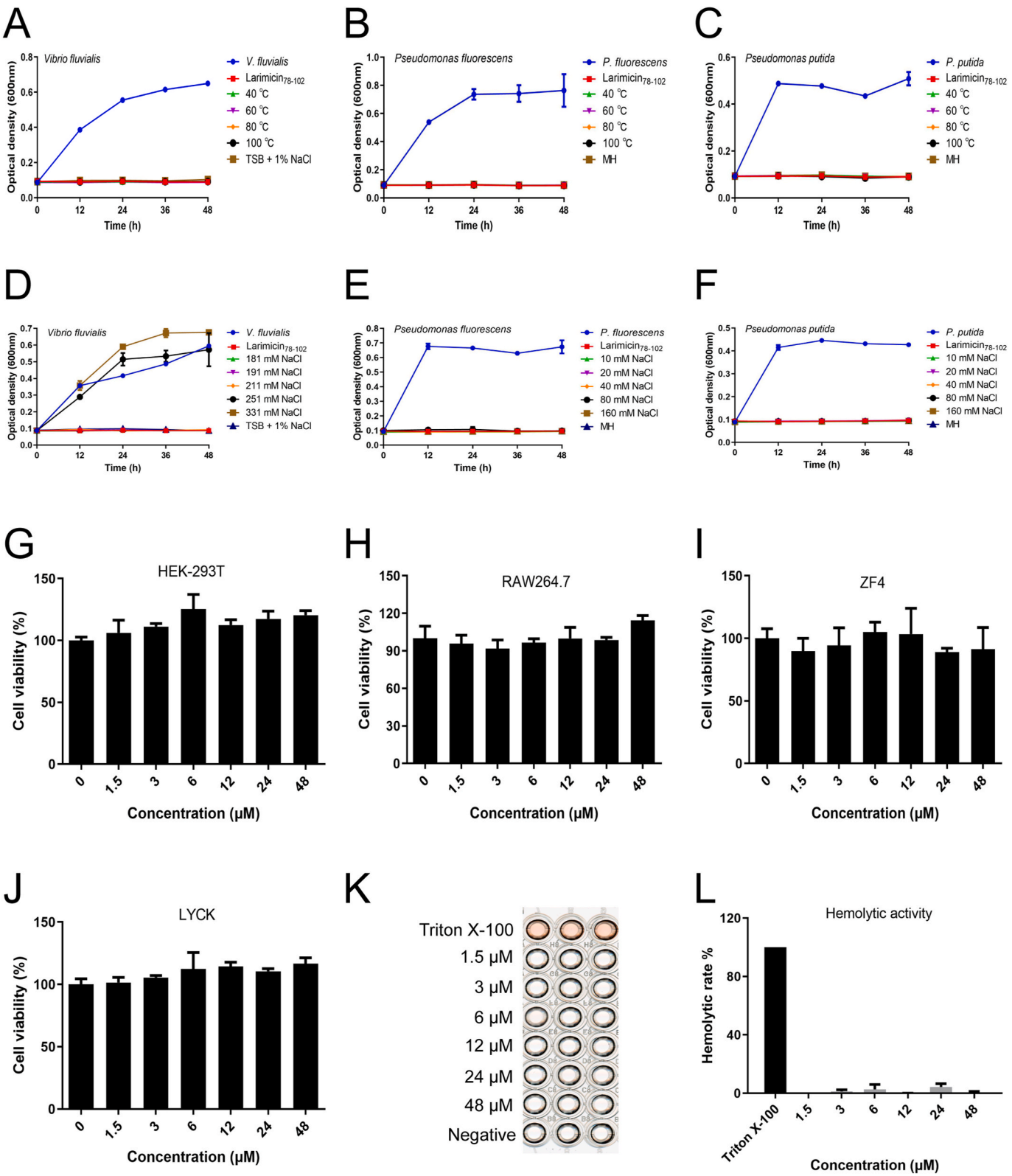

Fig. 8. The thermal stability of Larimicin$_{78\text{-}102}$. *V. fluvialis* (A), *P. fluorescens* (B), and *P. putida* (C) were exposed to heat-treated Larimicin$_{78\text{-}102}$. The antimicrobial activity of Larimicin$_{78\text{-}102}$ against *V. fluvialis* (D), *P. fluorescens* (E), and *P. putida* (F) under different NaCl concentrations. The cytotoxicity of Larimicin$_{78\text{-}102}$ on HEK-293T (G), RAW264.7 (H), ZF4 (I), and LYCK (J) cell lines. Hemolytic activity of Larimicin$_{78\text{-}102}$ on mouse erythrocytes (K and L).

conditions, such as cations, serum, and proteases, leading to diminished or lost efficacy [50,51]. We evaluated whether Larimicin$_{78\text{-}102}$ would be affected by various factors. In the present study, Larimicin$_{78\text{-}102}$ maintained potent antimicrobial activity after heating at 100 °C for 30 min, indicating good thermal stability. This is consistent with earlier findings for HSEP3 [52] and BAMP [53], both of which maintained strong antimicrobial activity across different temperature ranges. Furthermore, AMPs preferentially act on bacterial membranes through electrostatic

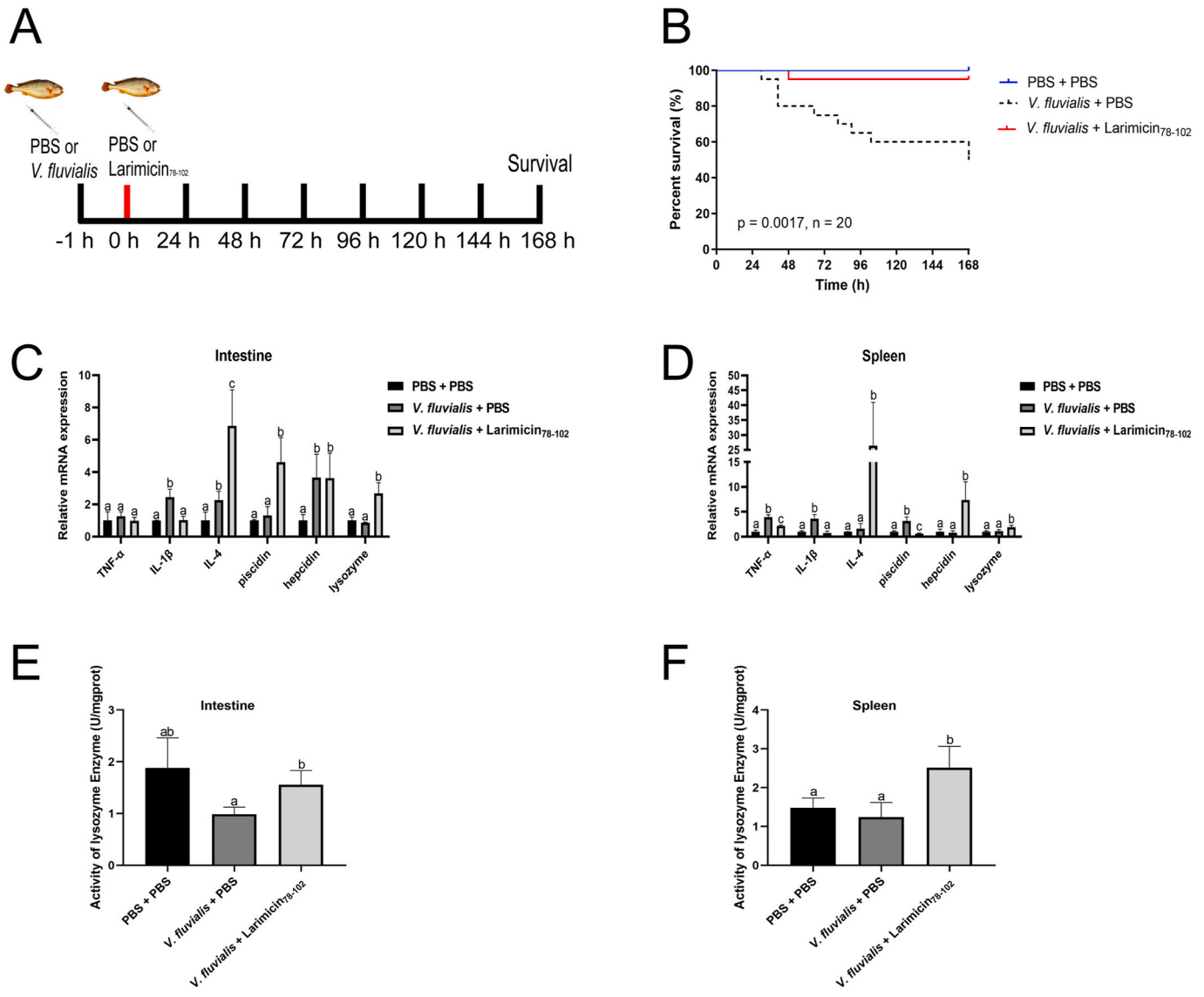

Fig. 9. Anti-*V. fluvialis* infective effect of Larimicin$_{78\text{-}102}$ *in vivo*. (A) A schematic diagram of *V. fluvialis* infection in large yellow croaker. (B) The anti-*V. fluvialis* infective effect of Larimicin$_{78\text{-}102}$ in large yellow croaker. Kaplan–Meier log-rank testing was used to analyze the survival curve. The expression levels of immune-related genes in the intestine (C) and spleen (D). The enzymatic activity of lysozyme in the intestine (E) and spleen (F). Differences were considered statistically significant at $p < 0.05$. (For interpretation of the references to color in this figure legend, the reader is referred to the Web version of this article.)

binding [54]. However, high concentrations of cations influence the electrostatic binding of AMPs, thus affecting their antimicrobial activity [54]. Our results showed that Larimicin$_{78\text{-}102}$ maintained its antimicrobial efficacy against *P. fluorescens* and *P. putida* in a 160 mM NaCl solution, and exhibited high cation tolerance against *V. fluvialis* in a 211 mM NaCl solution. Given that *V. fluvialis* grows in low-nutrient environments rich in inorganic salt ions, the high salinity tolerance of Larimicin$_{78\text{-}102}$ may be a key factor in its activity against *V. fluvialis*. The good thermal stability and high cation tolerance of Larimicin$_{78\text{-}102}$ lay the foundation for its future application in feed additives, aquatic drugs, and food preservation.

Another challenge in the application of AMPs is their cytotoxicity. Studies have shown that some AMPs, such as melittin, Hecate-βCG, and arenicins, can be toxic to vertebrate cells [55–57]. No toxicity is a prerequisite for the application of AMPs in various contexts. In this study, Larimicin$_{78\text{-}102}$ showed no cytotoxicity to vertebrate cells (HEK-293T, RAW264.7, ZF4, and LYCK) and exhibited no hemolytic activity to mouse erythrocytes, suggesting good biocompatibility. This suggested that Larimicin$_{78\text{-}102}$ would be safe and effective for *in vivo* use. Subsequently, the *in vivo* efficacy of Larimicin$_{78\text{-}102}$ was evaluated using a large yellow croaker model infected with *V. fluvialis*. *V. fluvialis*, a halophilic Gram-negative bacterium, can be sourced from water, animal feces and seafood [58]. It is an important cause of cholera-like bloody diarrhea, which can lead to wound infections and primary sepsis [58, 59]. Our findings indicated that Larimicin$_{78\text{-}102}$ effectively combated *V. fluvialis in vivo*. It significantly improved the survival of large yellow croakers, suggesting a pronounced *in vivo* anti-*V. fluvialis* effect.

Previous research has established that AMPs not only possess direct bactericidal activity but also play important roles in immunomodulation and inflammatory responses, helping to control bacterial infections in aquatic organisms [60]. Immune factors, including pro-inflammatory cytokines, anti-inflammatory factors, and immune genes such as *hepcidin* and *β-defensin*, play an important role in the inflammatory response triggered by bacterial infection [61,62]. In the present study, the pro-inflammatory factors *TNF-α* and *IL-1β* were obviously elevated after *V. fluvialis* infection. *IL-1β* exhibits potent pro-inflammatory activity, triggering an acute phase response and ultimately leading to widespread inflammation [63]. *TNF-α* has pro-inflammatory activity and is

associated with various diseases, including autoimmune disorders and inflammatory bowel disease [64,65]. Exposure to Larimicin$_{78\text{-}102}$ significantly reduced the levels of *TNF-α* and *IL-1β*, while enhancing the expression of *IL-4*, *piscidin*, *hepcidin* and *lysozyme*. It also increased the enzymatic activity of lysozyme to further exert bactericidal effects *in vivo*. *IL-4* serves as an anti-inflammatory mediator that effectively reduces the production of pro-inflammatory factors (*TNF-α* and *IL-1β*), making it vital for the treatment of autoimmune and inflammatory diseases [66]. The concentration of AMPs is generally low under normal physiological conditions, but their production substantially increases during pathogen invasion and inflammation, promoting antimicrobial activity [67]. This demonstrates that Larimicin$_{78\text{-}102}$ administration can prevent excessive inflammation and boost antibacterial activity. These findings confirmed that Larimicin$_{78\text{-}102}$ improved the survival rate of large yellow croaker challenged with *V. fluvialis* by effectively regulating the immune response. These results provided new insights into controlling *V. fluvialis* infection in aquaculture, and Larimicin$_{78\text{-}102}$ is expected to be an effective and green anti-*V. fluvialis* agents in aquaculture.

In summary, a novel immune-associated functional gene, named *Larimicin*, was identified from large yellow croaker, and its full-length cDNA sequence was obtained. *Larimicin* gene was widely distributed in various tissues and significantly up-regulated in the liver after exposure to *V. alginolyticus* or *V. parahaemolyticus*. A novel AMP, Larimicin$_{78\text{-}102}$, was further screened from *Larimicin* and exhibited broad-spectrum antimicrobial efficacy. Larimicin$_{78\text{-}102}$ disrupted the cell membranes of *V. fluvialis*, *P. fluorescens*, and *P. putida*, increasing membrane permeability, inducing ATP release and ROS accumulation, ultimately leading to bacterial death. Larimicin$_{78\text{-}102}$ showed no cytotoxicity and no obvious hemolytic activity. Notably, Larimicin$_{78\text{-}102}$ significantly improved the survival of large yellow croaker under *V. fluvialis* challenge. It suppressed the expression of two pro-inflammatory factors *TNF-α* and *IL-1β*, increased the mRNA level of the anti-inflammatory factor *IL-4*, as well as up-regulated the transcription levels of *piscidin*, *hepcidin*, and *lysozyme*. Additionally, it enhanced the enzymatic activity of lysozyme. This study explored the *in vitro* antimicrobial activity of Larimicin$_{78\text{-}102}$ against *V. fluvialis* and its *in vivo* anti-infective effects, highlighting its potential as a marine-derived AMP for the development of anti-*V. fluvialis* drugs in aquaculture.

CRediT authorship contribution statement

Zhenzhen Zhou: Writing – original draft, Investigation, Methodology, Visualization, Software, Data curation, Formal analysis. **Fangyi Chen:** Writing – review & editing, Supervision, Project administration, Funding acquisition, Conceptualization. **Hua Hao:** Investigation. **Kejian Wang:** Writing – review & editing, Supervision, Project administration, Funding acquisition, Conceptualization.

Ethical approval

This animal study was approved by the Laboratory Animal Management and Ethics Committee of Xiamen University. All animal experiments were conducted in strict accordance with the regulations of Xiamen University.

Declaration of competing interest

The authors declare that there were no commercial or financial relationships present during the research that could be considered a potential conflict of interest.

Acknowledgments

This research was funded by several grants, including the National Natural Science Foundation of China (grant numbers 42376089), Fujian Ocean and Fisheries Bureau (grant FJHY-YYKJ-2022-1-14), Fujian Ocean Synergy Alliance (grant FOCAL2023-0207), Xiamen Ocean Development Bureau (grant number 22CZP002HJ08) and Pingtan Research Institute of Xiamen University (grant number Z20220743). We also express our gratitude to laboratory engineers Zhiyong Lin, Hui Peng, Huiyun Chen and Ming Xiong for their technical assistance throughout the study.

Appendix A. Supplementary data

Supplementary data to this article can be found online at https://doi.org/10.1016/j.fsi.2025.110279.

Data availability

The authors do not have permission to share data.

References

[1] L. Liu, M. Ge, X. Zheng, Z. Tao, S. Zhou, G. Wang, Investigation of Vibrio alginolyticus, V. harveyi, and V. parahaemolyticus in large yellow croaker, Pseudosciaena crocea (Richardson) reared in Xiangshan Bay, China, Aquac. Rep. 3 (2016) 220–224. Complete.
[2] J.T. Zhang, S.M. Zhou, S.W. An, L. Chen, G.L. Wang, Visceral granulomas in farmed large yellow croaker, Larimichthys crocea (Richardson), caused by a bacterial pathogen, Pseudomonas plecoglossicida, J. Fish. Dis. 37 (2) (2014) 113–121.
[3] E.O. Igbinosa, A.I. Okoh, Antibiotic susceptibility profiles of some Vibrio strains isolated from wastewater final effluents in a rural community of the Eastern Cape Province of South Africa, BMC Microbiol. 10 (2010) 143.
[4] D.F. Mello, R. Trevisan, N.M. Danielli, A.L. Dafre, Vulnerability of glutathione-depleted Crassostrea gigas oysters to Vibrio species, Mar. Environ. Res. 154 (2020) 104870.
[5] F. Mao, K. Liu, N.K. Wong, X. Zhang, W. Yi, Z. Xiang, S. Xiao, Z. Yu, Y. Zhang, Virulence of Vibrio alginolyticus accentuates apoptosis and immune rigor in the oyster Crassostrea hongkongensis, Front. Immunol. 12 (2021) 746017.
[6] T. Marudhupandi, T.T.A. Kumar, S. Prakash, J. Balamurugan, N.B. Dhayanithi, Vibrio parahaemolyticus a causative bacterium for tail rot disease in ornamental fish, Amphiprion sebae, Aquac. Rep. 8 (2017) 39–44.
[7] C. Jian, Preliminary studies on a pathogen of vibriosis of cultured Paralichthys olivaceus, Marine Fisherries Res. (1) (2001) 37–41.
[8] Z.Z. Xia, S.Y. Quan, W. Jun, Y.Q. Pi, M.A. Liangdepartmentofoceanogrophy, XiamenUniversity, xiamen, China, studies on the pathogen of Penaeus monodon Vibrio fluvialis Type I. Acta Scientiarum Naturalium Universitatis Sunyatseni, 2000, pp. 208–213.
[9] Z. Su-Qin, J.I. Rong-Xing, S.U. Yong-Quan, W. Jun, Q. Ying-Xue, M.A. Ying, Z. Wen-Zheng, L.I. Hai-Ping, Y. Qing-Pi, Study on adhesion characteristics of Vibrio fluvialis to the gill mucus of Pseudosciaena crocea, Oceanol. Limnol. Sinica 43 (2) (2012) 389–393.
[10] A.B. Kahla-Nakbi, K. Chaieb, A. Besbes, T. Zmantar, A. Bakhrouf, Virulence and enterobacterial repetitive intergenic consensus PCR of Vibrio alginolyticus strains isolated from Tunisian cultured gilthead sea bream and sea bass outbreaks, Vet. Microbiol. 117 (2–4) (2006) 321–327.
[11] B. Ye, S.L. Li, Q. Fan, Z.J. Zhao, P.P. Li, D.M. Yue, X.D. Wang, Y. Dong, D.N. Liu, Z. C. Zhou, Antimicrobial activity of a novel moricin-like peptide from the Chinese oak silkworm against Vibrio pathogens in sea cucumbers, Aquac. Rep. 35 (2024) 102010.
[12] N. Mohamad, Mohammad Noor AzmaiYasin, Ina Salwany MdSaad, Mohd ZamriNasruddin, Nurrul ShaqinahAl-saari, NurhidayuMino, SayakaSawabe, Tomoo, Vibriosis in cultured marine fishes: a review, Aquaculture 512 (2019) 734289.
[13] E. Harpeni, A. Isnansetyo, I. Istiqomah, Murwantoko, Bacterial biocontrol of vibriosis in shrimp: a review, Aquac. Int. 32 (5) (2024) 5801–5831.
[14] B.D. Ulery, SNAPPy solution for fighting drug-resistant bacteria, Sci. Transl. Med. 8 (360) (2016), 360ec164-360ec164.
[15] M. Magana, M. Pushpanathan, A.L. Santos, L. Leanse, G.P. Tegos, The value of antimicrobial peptides in the age of resistance, Lancet Infect. Dis. 20 (9) (2020) e216–e230.
[16] H.X. Luong, T.T. Thanh, T.H. Tran, Antimicrobial peptides - advances in development of therapeutic applications, Life Sci. 260 (2020) 118407.
[17] S.H. White, W.C. Wimley, Hydrophobic interactions of peptides with membrane interfaces, Biochim. Biophys. Acta 1376 (3) (1998) 339–352.
[18] Q. Wu, J. Patočka, K. Kuča, Insect antimicrobial peptides, a mini review, Toxins 10 (11) (2018) 461.
[19] S. Ji, F. An, T. Zhang, M. Lou, J. Guo, K. Liu, Y. Zhu, J. Wu, R. Wu, Antimicrobial peptides: an alternative to traditional antibiotics, Eur. J. Med. Chem. 265 (2024) 116072.
[20] X. Wang, X. Hong, F. Chen, K.J. Wang, A truncated peptide Spgillcin(177-189) derived from mud crab Scylla paramamosain exerting multiple antibacterial activities, Front. Cell. Infect. Microbiol. 12 (2022) 928220.
[21] J. Andy, Tincu, W. Steven, Taylor, Antimicrobial peptides from marine invertebrates, Antimicrob. Agents Chemother. 48 (10) (2004) 3645–3654.

[22] R. Chen, Y. Mao, J. Wang, M. Liu, Y. Qiao, L. Zheng, Y. Su, Q. Ke, W. Zheng, Molecular mechanisms of an antimicrobial peptide piscidin (Lc-pis) in a parasitic protozoan, Cryptocaryon irritans, BMC Genom. 19 (1) (2018) 192.
[23] K.J. Wang, J.J. Cai, L. Cai, H.D. Qu, M. Yang, M. Zhang, Cloning and expression of a hepcidin gene from a marine fish (Pseudosciaena crocea) and the antimicrobial activity of its synthetic peptide, Peptides 30 (4) (2009) 638–646.
[24] K. Li, Wanru, Xiaojuan Chen, Tian Luo, Yinnan Mu, Xinhua Chen, Molecular and functional identification of a beta-defensin homolog in large yellow croaker (Larimichthys crocea), J. Fish. Dis. 44 (4) (2021) 391–400.
[25] Q.J. Zhou, J. Wang, M. Liu, Y. Qiao, W.S. Hong, Y.Q. Su, K.H. Han, Q.Z. Ke, W. Q. Zheng, Identification, expression and antibacterial activities of an antimicrobial peptide NK-lysin from a marine fish Larimichthys crocea, Fish Shellfish Immunol. 55 (2016) 195–202.
[26] Y. Libing Zheng, J. Li, Y. Wang, J. Pan, W. Chen, L. Zheng, Lin, Antibacterial and antiparasitic activities analysis of a hepcidinlike antimicrobial peptide from Larimichthys crocea, Acta Oceanol. Sin. 39 (10) (2020) 133–143.
[27] Z. Shan, K. Zhu, H. Peng, B. Chen, J. Liu, F. Chen, X. Ma, S. Wang, K. Qiao, K. Wang, The new antimicrobial peptide SpHyastatin from the mud crab Scylla paramamosain with multiple antimicrobial mechanisms and high effect on bacterial infection, Front. Microbiol. 7 (67) (2016) 1140.
[28] Y.C. Chen, Y. Yang, C. Zhang, H.Y. Chen, F. Chen, K.J. Wang, A novel antimicrobial peptide sparamosin(26-54) from the mud crab Scylla paramamosain showing potent antifungal activity against Cryptococcus neoformans, Front. Microbiol. 12 (2021) 746006.
[29] A.J. Moyano, C.R. Mas, C.A. Colque, A.M. Smania, Dealing with biofilms of Pseudomonas aeruginosa and Staphylococcus aureus : in vitro evaluation of a novel aerosol formulation of silver sulfadiazine, Burns 46 (1) (2020) 128–135.
[30] H.M. Chen, S.C. Chan, J.C. Lee, C.C. Chang, R.W. Jack, Transmission electron microscopic observations of membrane effects of antibiotic cecropin B on Escherichia coli, Microsc. Res. Tech. 62 (5) (2003) 423.
[31] O.N. Silva, M.D.T. Torres, J. Cao, E.S.F. Alves, C.D.L. Fuente-Nunez, Repurposing a peptide toxin from wasp venom into antiinfectives with dual antimicrobial and immunomodulatory properties, Proc. Natl. Acad. Sci. USA 117 (43) (2020) 26936–26945.
[32] V. Mayandi, Q. Xi, E.T. Leng, S.K. Koh, T.Y. Jie, V.A. Barathi, M.H. Urf Turabe Fazil, M.L. Somaraju Chalasani, J. Varadarajan, D.S.J. Ting, R.W. Beuerman, L. W. Chan, R. Agrawal, T.M. Sebastian, L. Zhou, N.K. Verma, R. Lakshminarayanan, Rational substitution of epsilon-lysine for alpha-lysine enhances the cell and membrane selectivity of pore-forming melittin, J. Med. Chem. 63 (7) (2020) 3522–3537.
[33] D. Zhu, F. Chen, Y.C. Chen, H. Peng, K.J. Wang, The long-term effect of a nine amino-acid antimicrobial peptide AS-hepc3(48-56) against Pseudomonas aeruginosa with No detectable resistance, Front. Cell. Infect. Microbiol. 11 (2021) 955.
[34] S. Halder, K.K. Yadav, R. Sarkar, S. Mukherjee, P. Saha, S. Haldar, S. Karmakar, T. Sen, Alteration of Zeta potential and membrane permeability in bacteria: a study with cationic agents, SpringerPlus 4 (2015) 672.
[35] S. He, Z. Yang, X. Li, H. Wu, L. Zhang, A. Shan, J. Wang, Boosting stability and therapeutic potential of proteolysis-resistant antimicrobial peptides by end-tagging β-naphthylalanine, Acta Biomater. 164 (2023) 175–194.
[36] T. Zheng, G. Wang, S. Jin, Prevention and cure of vibriosis in aquatic animals: a review, J. Oceanogr. Taiwan Strait (3) (2002) 372–378.
[37] J. Ao, Y. Mu, L.X. Xiang, D. Fan, M. Feng, S. Zhang, Q. Shi, L.Y. Zhu, T. Li, Y. Ding, Genome sequencing of the perciform fish Larimichthys crocea provides insights into molecular and genetic mechanisms of stress adaptation, Sci. Found. China 11 (4) (2015) e1005118.
[38] D. Rajme-Manzur, T. Gollas-Galván, F. Vargas-Albores, M. Martínez-Porchas, M. n. Hernández-Oate, J. Hernández-López, Granulomatous bacterial diseases in fish: an overview of the host's immune response, Comp. Biochem. Physiol. Mol. Integr. Physiol. 261 (2021) 111058.
[39] P.R. Rauta, B. Nayak, S. Das, Immune system and immune responses in fish and their role in comparative immunity study: a model for higher organisms, Immunol. Lett. 148 (1) (2012) 23–33.
[40] J. Su, H. Li, J. Hu, D. Wang, F. Zhang, Z. Fu, F. Han, LcCCL28-25, derived from piscine chemokine, exhibits antimicrobial activity against gram-negative and gram-positive bacteria in vitro and in vivo, Microbiol. Spectr. 10 (3) (2022) e0251521.
[41] V. Teixeira, M.J. Feio, M. Bastos, Role of lipids in the interaction of antimicrobial peptides with membranes, Prog. Lipid Res. 51 (2) (2012) 149–177.
[42] A. Li, C. Shi, S. Qian, Z. Wang, S. Zhao, Y. Liu, Z. Xue, Evaluation of antibiotic combination of litsea cubeba essential oil on Vibrio parahaemolyticus inhibition mechanism and anti-biofilm ability, Soc. Sci. Electr. Pub. 168 (2022) 105574.
[43] M. Ashrafudoulla, M.F.R. Mizan, J.W. Ha, S.H. Park, S.D. Ha, Antibacterial and antibiofilm mechanism of eugenol against antibiotic resistance Vibrio parahaemolyticus, Food Microbiol. 91 (2020) 103500.
[44] M. Hossain, A.M. Ibne Momen, A. Rahman, J. Biswas, M. Yasmin, J. Nessa, C. R. Ahsan, Draft-genome analysis provides insights into the virulence properties and genome plasticity of Vibrio fluvialis organisms isolated from shrimp farms and Turag river in Bangladesh, Arch. Microbiol. 204 (8) (2022) 527.
[45] J. Park, J.H. Oh, H.K. Kang, M.C. Choi, C.H. Seo, Y. Park, Scorpion-Venom-derived antimicrobial peptide Css54 exerts potent antimicrobial activity by disrupting bacterial membrane of zoonotic bacteria, Antibiotics 9 (11) (2020) 831.
[46] Y.C. Chen, W. Qiu, W. Zhang, J. Zhang, R. Chen, F. Chen, K.J. Wang, A novel antimicrobial peptide sp-LECin with broad-spectrum antimicrobial activity and anti-Pseudomonas aeruginosa infection in zebrafish, Int. J. Mol. Sci. 24 (1) (2022) 267.
[47] Z. He, Q. Xu, B. Newland, R. Foley, I. Lara-Sáez, J.F. Curtin, W. Wang, Reactive oxygen species (ROS): utilizing injectable antioxidative hydrogels and ROS-producing therapies to manage the double-edged sword, J. Mater. Chem. B 9 (32) (2021) 6326–6346.
[48] B. Ezraty, A. Gennaris, F. Barras, J.F. Collet, Oxidative stress, protein damage and repair in bacteria, Nat. Rev. Microbiol. 15 (7) (2017) 385–396.
[49] B. Lee, J.S. Hwang, D.G. Lee, Antibacterial action of lactoferricin B like peptide against Escherichia coli: reactive oxygen species-induced apoptosis-like death, J. Appl. Microbiol. 129 (2) (2020) 287–295.
[50] F. Annarita, L. Lucia, F. Gianluigi, V. Mariateresa, I. Maria, M. Giancarlo, G. Massimiliano, G. Stefania, Marine antimicrobial peptides: nature provides templates for the design of novel compounds against pathogenic bacteria, Int. J. Mol. Sci. 17 (5) (2016) 785.
[51] M.T.C. McCrudden, D.T.F. Mclean, M. Zhou, J. Shaw, G.J. Linden, C.R. Irwin, F. T. Lundy, The host defence peptide LL-37 is susceptible to proteolytic degradation by wound fluid isolated from foot ulcers of diabetic patients, Int. J. Pept. Res. Therapeut. 20 (4) (2014) 457–464.
[52] Y.L. Vishweshwaraiah, A. Acharya, V. Hegde, B. Prakash, Rational design of hyperstable antibacterial peptides for food preservation, NPJ Sci. Food 5 (1) (2021) 26.
[53] S. Choyam, P.M. Jain, R. Kammara, Characterization of a potent new-generation antimicrobial peptide of, Front. Microbiol. 12 (2021) 710741.
[54] W. Xian, M.R. Hennefarth, M.W. Lee, T. Do, E.Y. Lee, A.N. Alexandrova, G.C. L. Wong, Histidine-Mediated ion specific effects enable salt tolerance of a pore-forming marine antimicrobial peptide, Angew. Chem. 61 (25) (2022) e202108501.
[55] N.R. Soman, S.L. Baldwin, G. Hu, J.N. Marsh, G.M. Lanza, J.E. Heuser, J.M. Arbeit, S.A. Wickline, P.H. Schlesinger, Molecularly targeted nanocarriers deliver the cytolytic peptide melittin specifically to tumor cells in mice, reducing tumor growth, J. Clin. Investig. 119 (9) (2009) 2830–2842.
[56] H. William, E. Fred, L. Carola, Destruction of breast cancers and their metastases by lytic peptide conjugates in vitro and in vivo, Mol. Cell. Endocrinol. 260–262 (1) (2007) 183–189.
[57] Mikhail Yu Myshkin, Pavel V. Panteleev, Zakhar Shenkarev, O. Ovchinnikova, Dimerization of the antimicrobial peptide arenicin plays a key role in the cytotoxicity but not in the antibacterial activity, Biochem. Biophys. Res. Commun. 482 (4) (2017) 1320–1326.
[58] E.O. Igbinosa, A.I. Okoh, Vibrio fluvialis: an unusual enteric pathogen of increasing public health concern, Int. J. Environ. Res. Publ. Health 7 (10) (2010) 3628–3643.
[59] T. Takezawa, N. Matsunaga, A. Miki, T. Arizumi, A. Tanaka, F. Ito, S. Kawachi, Vibrio fluvialis bacteremia in an immunocompetent patient with acute cholangitis, Intern. Med. 63 (22) (2024) 3101–3104.
[60] J. Ouyang, Y. Zhu, W. Hao, X. Wang, H. Yang, X. Deng, T. Feng, Y. Huang, H. Yu, Y. Wang, Three naturally occurring host defense peptides protect largemouth bass (Micropterus salmoides) against bacterial infections, Aquaculture 546 (2022) 737383.
[61] P. Wang, M.Z. Zhu, W. Huang, C.F. Huang, S. Wilson, Lysicamine in a Lotus leaves extract may Be responsible for antibacterial and anti-inflammation activity, Appl. Mech. Mater. 108 (2012) 189–193.
[62] E. Wirthgen, G. Domanska, Editorial: polarization of cellular immune response in the context of inflammation and cancer, Front. Immunol. 15 (2024) 1433808.
[63] Y. Wang, M. Che, J. Xin, Z. Zheng, S. Zhang, The role of IL-1β and TNF-α in intervertebral disc degeneration, Biomed. Pharmacother. 131 (2020) 110660.
[64] I. Dichamp, A. Bourgeois, C. Dirand, G. Herbein, D. Wendling, Increased nuclear factor-kappaB activation in peripheral blood monocytes of patients with rheumatoid arthritis is mediated primarily by tumor necrosis factor-alpha, J. Rheumatol. 34 (10) (2007) 1976–1983.
[65] J. Brynskov, P. Foegh, G. Pedersen, C. Ellervik, T. Kirkegaard, A. Bingham, T. Saermark, Tumour necrosis factor α converting enzyme (TACE) activity in the colonic mucosa of patients with inflammatory bowel disease, Gut 51 (1) (2002) 37.
[66] M. Akdis, S. Burgler, R. Crameri, T. Eiwegger, H. Fujita, E. Gomez, S. Klunker, N. Meyer, L. O'Mahony, O. Palomares, Interleukins, from 1 to 37, and interferon-γ: receptors, functions, and roles in diseases, J. Allergy Clin. Immunol. 127 (3) (2011) 701–721, e1-70.
[67] V.G. Arzumanyan, E.P. Bystritskaya, T.I. Kolyganova, A.M. Iksanova, P. V. Samoilikov, S.Y. Konanykhina, A.A. Vartanova, O.A. Svitich, Antimicrobial activity of the serum before and after vaccination with EpiVacCorona, Bull. Exp. Biol. Med. 173 (3) (2022) 354–360.